IEEE Access
Multidisciplinary | Rapid Review | Open Access Journal

Received 18 July 2025, accepted 30 July 2025, date of publication 11 August 2025, date of current version 21 August 2025.

Digital Object Identifier 10.1109/ACCESS.2025.3597579

RESEARCH ARTICLE

Adaptive Modulation for Non-Orthogonal Multiple Access (NOMA) With Imperfect SIC

MILAD HESHMATI[1], ALI H. BASTAMI[2], LOKMAN SBOUI[3], (Senior Member, IEEE), AND ZBIGNIEW DZIONG[1], (Senior Member, IEEE)

[1]Electrical Engineering Department, École de Technologie Supérieure (ÉTS), University of Québec, Montréal, QC H3C 1K3, Canada
[2]Faculty of Electrical Engineering, K. N. Toosi University of Technology, Tehran 1631714191, Iran
[3]Systems Engineering Department, École de Technologie Supérieure (ÉTS), University of Québec, Montréal, QC H3C 1K3, Canada

Corresponding author: Milad Heshmati (milad.heshmati.1@ens.etsmtl.ca)

This work was supported in part by the Natural Sciences and Engineering Research Council of Canada (NSERC) under Grant RGPIN-2020-06520.

ABSTRACT The increasing demand for high-capacity wireless communications has always been a challenge for researchers. Non-Orthogonal Multiple Access (NOMA) is one of the emerging schemes that can improve the capacity of wireless networks. In the power-domain NOMA, users share the same frequency and time but with different power levels. In this paper, we propose a novel adaptive modulation scheme for a NOMA-based wireless network to achieve better throughput efficiency and improve the system spectral efficiency by considering imperfect Successive Interference Cancellation (SIC). This scheme allocates the appropriate modulation orders by solving an optimization problem constrained by a maximum Bit Error Rate (BER). We investigate the BER and throughput calculations to assess the efficacy of the proposed scheme. The results show that our adaptive scheme greatly improves the spectral efficiency compared to the traditional fixed modulation NOMA systems, indicating its potential to satisfy the demanding performance standards of future wireless networks.

INDEX TERMS Adaptive modulation, Nakagami fading, NOMA.

I. INTRODUCTION

In the fifth generation (5G) of wireless networks, in order to improve the capacity and quality of service, multiple access techniques are being used, and these techniques can be very good candidates for implementation in the sixth generation (6G) of wireless networks as well. One of the most promising techniques which is investigated vastly by researchers these days is non-orthogonal multiple access (NOMA). In this scheme, two or more nodes in the network use the same frequency at the same time but the users are differentiable by their signal power level or their code.

In the power-domain NOMA, the transmitter combines the signals of different users by assigning them specific power allocation coefficients. The resulting signal is a weighted sum of the users' signals, and this process is called Superposition Coding (SC). Let us consider a NOMA network with one base station (BS) and two users, the Far User (FU) and the Near User (NU). Based on the principles of NOMA, the power of the FU signal is greater than that of the NU signal. Accordingly, the FU decodes its signal by considering the NU signal as noise. On the other hand, the NU first performs Successive Interference Cancellation (SIC) to remove the effects of the FU signal and then decodes its own signal. For simplicity of the analysis, the SIC can be considered perfect [1], [2]. However, in practice, the SIC detectors are not ideal and result in imperfect SIC. Moreover, the SIC detectors have some delay because the n-th user should decode $n-1$ other user signals in order to obtain its own message [3]. Recent studies examine imperfect SIC in RIS-partition NOMA [4], reliable QAM-based power allocation [5], hybrid SIC success under Rayleigh fading [6], multi-group MIMO-NOMA precoding with residual SIC analysis [7], and hardware-impaired MISO-NOMA signaling [8].

A. RELATED WORKS

Channel fading increases the Bit Error Rate (BER), and several methods can be employed to mitigate its effects, such

The associate editor coordinating the review of this manuscript and approving it for publication was Claudia Raibulet.

as increasing transmission power or applying channel coding and diversity techniques [9]. However, these methods are designed for the worst-case scenario and do not utilize the maximum capacity of the channel in all states. In addition, the interference caused by the nature of the NOMA system downgrades the condition of the receivers as they need to tackle this interference before detecting their signals. Moreover, NOMA-based systems typically use a fixed modulation scheme, which can lead to inefficiencies as network conditions improve for users or even when their channel conditions degrade. This reduces the maximum achievable rate when the status of the channel is better than the system design and increases the BER as it gets worse. Therefore, a method is needed to address these challenges and enhance the system efficiency under varying network conditions. In this paper, we address these issues by considering the dynamicity of the channel states in order to have the optimum throughput and maintain the desirable BER.

The BER analysis for the NOMA-based networks has recently attracted considerable attention in the literature. For instance, in [10], the performance of a NOMA wireless system is evaluated from a BER perspective. The system consists of two or three users who utilize Quadrature Phase Shift Keying (QPSK) modulations. However, the derived equations are not useful for higher-order modulations. In addition, the authors did not provide the closed-form equations for each combination of the system Modes and the final BER equations are expressed as a function of the complementary error function (Q function). In [11], the BER performance of a NOMA network consisting of three users is investigated. The results are only valid for QPSK modulation. In [12], the BER analysis for the downlink and uplink of a NOMA system is presented for the Binary Phase-Shift Keying (BPSK) and QPSK modulations. In [13], the BER for the downlink of a NOMA-based network with N users is calculated for BPSK modulation. In [14], the exact BER for NOMA-based Visible Light Communication (VLC) systems is provided.

There are options other than NOMA that can also be considered. If the channel fading is known for the transmitter, the Shannon capacity of the channel is achievable using adapting transmitter power, rate, coding, and modulation [15]. Using this concept, an approach was presented using adaptive rate and power for a network utilizing M-Quadrature Amplitude Modulation (MQAM) [16]. Due to increasing demand for data traffic, 6G telecommunication systems are not just a developed version of 5G [17], [18]. It consists of services and applications like IoT, automatic anomaly detection using machine learning approaches, and agricultural uses by means of cloud services. In 5G, multiple access schemes such as Orthogonal Frequency-Division Multiple Access (OFDMA), which consists of orthogonal frequency division, are utilized [19], [20]. Orthogonal Multiple Access (OMA) schemes are working well; however, they are incapable of supporting huge networks with various service requests [21]. This is because of limitations in Degrees of Freedom (DoF) which make the service unavailable for users with poor channel status until they have a proper state.

B. MOTIVATION AND CONTRIBUTION

In this paper, we propose a new adaptive modulation system for a NOMA-based network that includes one BS that serves two paired users, NU and FU, in each frequency beam. In this method, the modulation order of the signals for each user is first determined based on the Channel State Information (CSI) and then it is transmitted to both users. As a result, with improvements in the channel conditions of a user, the higher modulation order can be utilized to have the maximum available throughput. Moreover, under poor channel condition, the adaptive system reduces the modulation orders to maintain the maximum acceptable BER which is the constraint of the problem. In order to have realistic results close to the practical systems, we consider the SIC process to be non-ideal. Moreover, the exact BER for each user is derived which is crucial for the proposed system.

The main idea of adaptive transmission is to adjust the modulation order continuously to match the current situation of the channel with the transmission constraints. These parameters can be power, rate, modulation order, coding, or any combination of them [22], [23], [24], [25], [26], [27], [28], [29]. Therefore, without power loss or violating the BER constraint, using the variable nature of the wireless telecommunication networks, adaptive methods can adjust the parameters based on the instantaneous CSI. In other words, in a desirable channel state, the system operates with higher rates, and lower rates are used when the channel state becomes worse. For instance, if a NOMA system sets 4-QAM modulation for two users, as the channel state becomes better, it is possible to use higher-order QAM modulations for users and vice versa. Therefore, the proposed adaptive modulation scheme significantly enhances spectral efficiency in wireless telecommunication networks, particularly under dynamically changing user positions. According to the knowledge of the authors, the concept of adaptive modulation in NOMA networks was not used so far. In the following, for the sake of simplicity, different combinations of QAM modulation for NU and FU are defined as system Modes (also referred to as operational modes).

The main contributions of this paper are summarized as follows:

- Exact BER derivations for different system Modes with different channel statuses for each user.
- Considering the imperfect SIC in the system model and comparing it with the perfect SIC.
- Introducing an adaptive modulation system in a NOMA network where the modulation order for nodes can be changed dynamically.
- Employing the Nakagami distribution assumption along with Gamma function calculations to accurately model channel fading and derive closed-form performance metrics.

- Conducting an extensive throughput analysis to quantify the spectral efficiency improvements achieved by the adaptive modulation scheme under dynamic user scenarios.

The rest of the paper is organized as follows. In Section II, we discuss the system model used for this work. Error Probability Analysis is presented in Section III. Then the proposed adaptive modulation system for throughput maximization is investigated in Section IV. Section V analyzes the system performance in terms of the throughput, the average BER, and the average transmission rate. In Section VI, we provide the numerical results, and finally, the paper is concluded in Section VII.

II. SYSTEM MODEL

In this paper, we consider the downlink of a NOMA system where a BS employs adaptive modulation and superposition coding to serve two users over a Nakagami fading channel, while accounting for the effects of imperfect SIC. The BS is assumed to serve users in pairs, enabling efficient resource allocation and interference management. To increase the network capacity, the BS implements a NOMA scheme which implies that users must be sorted based on their distance to BS.

The system employs a single antenna for all transmitters and receivers. By leveraging channel estimation, users can be dynamically sorted based on their channel conditions, enabling more efficient allocation of resources. This can be achieved by solving an optimization problem under BER constraint which is presented in Section IV. Each frequency beam is allocated to two users who have good and bad channel states, named NU and FU, respectively. It is important to note that multiple node pairs exist in the network, each assigned as NU and FU. However, our analysis focuses on a single selected pair for the system model. Figure 1 depicts the structure of the proposed model.

FIGURE 1. System model for the proposed wireless network.

In the FU receiver, the NU symbol is treated as noise, allowing FU to detect its own symbol using Maximum Likelihood (ML) detection. This assumption is valid since higher power is assigned to the FU's symbol compared to the NU's symbol. The user with a better channel state (NU) performs SIC by first decoding and subtracting the FU symbol from the received signal to obtain its own signal for decoding.

At the BS, the weighted signals related to both users are being added to form the superimposed symbol. If we consider the NU signal as x_1 and the FU signal as x_2, therefore the resulting transmitted signal can be expressed as

$$x_{sc} = \sqrt{\varepsilon_1}x_1 + \sqrt{\varepsilon_2}x_2. \tag{1}$$

where x_{sc} shows the superimposed symbol, ε_1 and ε_2 are the assigned power to each user's signal. These powers are allocated as a percentage of the BS power. The division factor for this allocation is called α which is controlled by the NOMA system. For instance, $\alpha = 0.2$ means 20% of the BS power is allocated to NU and the rest 80% is assigned to FU. Therefore, considering P_s as the BS power, the assigned powers can be expressed as

$$\varepsilon_1 = \alpha P_s, \quad \varepsilon_2 = (1-\alpha)P_s. \tag{2}$$

Therefore, we can rewrite (1) as

$$x_{sc} = \sqrt{\alpha P_s}x_1 + \sqrt{(1-\alpha)P_{sx_2}}. \tag{3}$$

The superimposed signal x_{sc} is broadcasted to both NU and FU. The detection for each user is different since they need to extract their messages from the same signal using different methods. The FU extracts its own signal using ML and considers the NU signal as noise. At the NU receiver, the FU signal must be detected and then deducted from the received signal. After these steps, the NU reaches its own signal which can be detected. As it was mentioned before, this is the SIC process. Considering this, the received signal in the NU receiver can be expressed as

$$y_1 = h_1 x_{sc} + n_1 \tag{4}$$

where y_1 shows the received signal at the receiver, h_1 is the fading channel coefficient between BS and NU, and n_1 stands for Additive White Gaussian Noise (AWGN) with zero mean and variance N_0 at the NU receiver. It is supposed that the NU has a better channel state than FU. The user that has the better channel condition must do the SIC process. In this system, it is supposed that the SIC process is not ideal and it may have errors. Considering the practical environments and the fact that error in the SIC process will result in error propagation to the detection of the NU signal, considering non-ideal SIC becomes important. For the FU we have

$$y_2 = h_2 x_{sc} + n_2 \tag{5}$$

where y_2 shows the received signal at the receiver, h_2 is the channel coefficient between BS and FU, and n_2 stands for AWGN with zero mean and N_0 variance.

The BS uses QAM modulation for users with M_1 and M_2 modulation orders. It is supposed that the modulation for the user that has the better channel state must have greater or equal modulation order than the other user. For instance, if the modulation order for the FU is $M_2 = 2$, the modulation order for the NU can be $M_1 = 2$, $M_1 = 4$, or higher based on its channel state. Moreover, it is supposed that if the FU moves in a way that reaches a better channel state than the other user,

its label will be switched, and it will be considered as NU and it needs to do the SIC process as well. Therefore, in all cases, the NU must do the SIC process, and it is assumed that the symbol probabilities are equal.

As noted in [9] and [30], overlapping superimposed constellations in NOMA systems can degrade the performance of the SIC or ML detection. Our error analysis takes this into account by modeling the interference caused by overlapping symbols and its effect on the decoding process.

III. ERROR PROBABILITY ANALYSIS

In this section, we present the error probability analysis for the users' received signals. Different signal detection scenarios can result from allocating NU and FU different modulation orders because of the adaptive modulation technique. We describe these scenarios as "system Modes" to evaluate them methodically. Three system Modes are considered, and the error probabilities are shown as $P_{i,j}$ where $i = 1, \ldots, 3$ is the system Mode and $j = 1, 2$ expresses the NU and FU respectively.

We describe each system Mode in depth in the next subsections, with the formulations of the corresponding error probabilities.

A. FIRST SYSTEM MODE ($M_1 = 2, M_2 = 2$)

In the first system Mode, we investigate the BER for the users where BPSK modulation (referred to here as 2QAM for consistency in describing QAM schemes) is being used for both NU and FU. For this case, there are two available forms for the system. First, two constellations can be combined with each other on the same axis with different gains. In this case, the signaling will be as like (1). Since the signals are separated in their domain, therefore it can be depicted as in Figure 2.

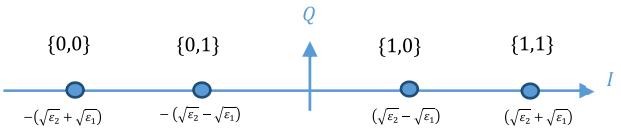

FIGURE 2. Inline combination of two 2QAM constellations.

In this case, FU detects its own message using the Q axis as a threshold to determine whether the bits are located at the left or right of the axis. If the bit is located on the right side, it will be considered as 1 and otherwise 0. On the other hand, NU must first determine the sign of $\pm\sqrt{\varepsilon_2}$ based on FU's symbol. Once identified, either $+\sqrt{\varepsilon_2}$ or $-\sqrt{\varepsilon_2}$ is subtracted from the received symbol, allowing NU to accurately detect its own message. As can be seen, the NU's signal is considered as noise for the detection process. Considering the complexity of this signaling and the additional noise, we propose another signaling for this Mode where two set of symbols are superimposed orthogonally.

In the other case, as it can be seen in Figure 3, we consider the NU and FU signals to be orthogonal. Therefore, the transmitted bits in the superposition constellation will be like

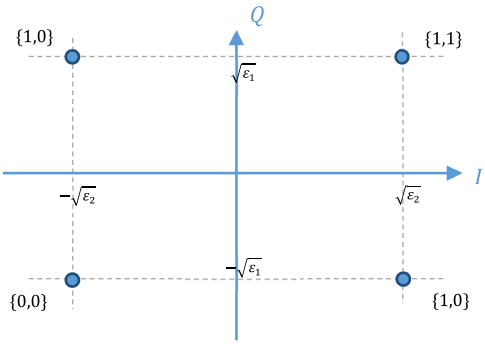

FIGURE 3. Orthogonal combination of two 2 QAMs.

$\{i_1, i_2\}$. In addition, the thresholds for NU and FU detection are I and Q axis respectively. Therefore, x_{sc} can be expressed as

$$x_{sc} = \sqrt{\varepsilon}_2 x_2 + j\sqrt{\varepsilon}_1 x_1 \tag{6}$$

where j denotes the in-phase part.

As observed from the constellation, the noise effect mentioned in the first case does not impact the detection of the other user's signal, as the signals remain orthogonal. In the following, we provide the exact BER derivation for both NU and FU.

1) FU BIT ERROR RATE

In order to calculate the FU BER, first, we should consider the condition where the errors might happen. Considering the second orthogonal case, the detection at FU is incorrect if

$$n_I \geq \sqrt{\varepsilon}_2 |h_2| \tag{7}$$

where n_I denotes the real part of the noise. Having this inequality, the error probability for FU can be calculated as

$$P_{1,2} = \Pr\left(n_I \geq \sqrt{\varepsilon}_2 |h_2|\right) \tag{8}$$

where $\Pr(.)$ stands for probability and the in-phase part of the noise (n_Q) does not impact this error probability. Considering the AWGN, this probability can be obtained as

$$P_{1,2}(e) = \mathrm{Q}\left(\sqrt{\frac{2\varepsilon_2 |h_2|^2}{N_0}}\right). \tag{9}$$

For this case, we can define the SNR variables as

$$\gamma_{1,A} = \frac{\varepsilon_2 |h_2|^2}{N_0}, \quad \overline{\gamma_{1,A}} = \frac{\varepsilon_2}{N_0} E\{|h_2|^2\} \tag{10}$$

where $E\{.\}$ is the expectation operator. Therefore, the BER expression can be rewritten as

$$P_{1,2}(e) = \mathrm{Q}(\sqrt{\gamma_{1,A}}). \tag{11}$$

To calculate the average BER for FU we can write

$$\overline{P_{1,2}(e)} = \int_0^\infty \mathrm{Q}(\sqrt{\gamma_{1,A}}) f_{\gamma_{1,A}}(\gamma_{1,A}) d\gamma_{1,A}. \tag{12}$$

For this system model, a frequency-nonselective fading model with the Nakagami distribution is considered. The Probability Density Function (PDF) of the Signal-to-Noise Ratio (SNR) for the Nakagami-m fading is given by

$$f_{\gamma_n}(\gamma_n) = \left(\frac{\Omega_n}{\overline{\gamma}_n}\right)^{\Omega_n} \frac{\gamma_n^{\Omega_n-1}}{\Gamma(\Omega_n)} e^{-\Omega_n\gamma_n/\overline{\gamma}_n}, \quad \gamma_n \geq 0 \tag{13}$$

where $\overline{\gamma}_n$ denotes the average of the SNR (γ_n) and Ω_n is the fading parameter. As a prerequisite for our derivation, we consider the following integrals from [31]:

$$\begin{aligned}
\mathcal{F}_1(\mathrm{t}_1,\mathrm{t}_2,\mathrm{t}_3,\mathrm{t}_4) &= \int_{t_3}^{t_4} \left(\frac{t_1}{t_2}\right)^{t_1} \frac{x^{t_1-1}}{\Gamma(t_1)} e^{-t_1x/t_2} dx, \\
\mathcal{F}_2(\mathrm{t}_1,\mathrm{t}_2,\mathrm{t}_3,\mathrm{t}_4,t_5) &= \frac{(t_1/t_2)^{t_1}}{\Gamma(t_1)} \int_{t_3}^{t_4} x^{t_1-1} e^{-\frac{t_1x}{t_2}} Q(t_5\sqrt{x}) dx, \\
\mathcal{F}_3(\mathrm{t}_1,\mathrm{t}_2,\mathrm{t}_3,\mathrm{t}_4,t_5,t_6) &= \int_{t_3}^{t_4} \frac{(t_1/t_2)^{t_1}}{\Gamma(t_1)} x^{t_1-1} e^{-\frac{t_1x}{t_2}} \\
&\quad \times Q(t_5\sqrt{x})Q(t_6\sqrt{x}) dx
\end{aligned} \tag{14}$$

where $\mathrm{t}_1, \mathrm{t}_2, \mathrm{t}_3, \mathrm{t}_4, t_5, t_6$ are the input parameters, $\Gamma(.)$ stands for the Gamma function and $\Gamma(.,.)$ is the Upper Incomplete Gamma function which is defined as [15]

$$\Gamma(\mathrm{t}_1,\mathrm{t}_2) = \int_{t_2}^{\infty} x^{t_1-1} e^{-x} dx. \tag{15}$$

Using the results in [31], the closed-form expressions for $\mathcal{F}_1$, $\mathcal{F}_2$ and $\mathcal{F}_3$ can be written as

$$\begin{aligned}
&\mathcal{F}_1(\mathrm{t}_1,\mathrm{t}_2,\mathrm{t}_3,\mathrm{t}_4) \\
&= \frac{1}{\Gamma(t_1)}\left[\Gamma\left(\mathrm{t}_1, \frac{\mathrm{t}_1\mathrm{t}_3}{\mathrm{t}_2}\right) - \Gamma\left(\mathrm{t}_1, \frac{\mathrm{t}_1\mathrm{t}_4}{\mathrm{t}_2}\right)\right], \\
&\mathcal{F}_2(\mathrm{t}_1,\mathrm{t}_2,\mathrm{t}_3,\mathrm{t}_4,t_5) \\
&= \frac{1}{12}\left(\frac{2t_1}{t_2t_5^2+2t_1}\right)^{t_1} \mathcal{F}_1\left(\mathrm{t}_1, \frac{2t_1t_2}{t_2t_5^2+2t_1}, \mathrm{t}_3, \mathrm{t}_4\right) \\
&\quad + \frac{1}{4}\left(\frac{3t_1}{2t_2t_5^2+3t_1}\right)^{t_1} \mathcal{F}_1\left(\mathrm{t}_1, \frac{3t_1t_2}{2t_2t_5^2+3t_1}, \mathrm{t}_3, \mathrm{t}_4\right), \\
&\mathcal{F}_3(\mathrm{t}_1,\mathrm{t}_2,\mathrm{t}_3,\mathrm{t}_4,t_5,t_6) \\
&= \frac{1}{12}\left(\frac{2t_1}{t_2t_6^2+2t_1}\right)^{t_1} \mathcal{F}_2\left(\mathrm{t}_1, \frac{2t_1t_2}{t_2t_5^2+2t_1}, \mathrm{t}_3, \mathrm{t}_4, t_5\right) \\
&\quad + \frac{1}{4}\left(\frac{3t_1}{2t_2t_6^2+3t_1}\right)^{t_1} \mathcal{F}_2\left(\mathrm{t}_1, \frac{3t_1t_2}{2t_2t_5^2+3t_1}, \mathrm{t}_3, \mathrm{t}_4, t_5\right).
\end{aligned} \tag{16}$$

Based on $\mathcal{F}_2$ and $\mathcal{F}_3$, let us define $\mathcal{H}_1$ and $\mathcal{H}_2$ as

$$\begin{aligned}
\mathcal{H}_1(\varphi) &\triangleq \mathcal{F}_2(\Omega_n, \overline{\gamma}_n, -\infty, +\infty, \varphi), \\
\mathcal{H}_2(\varphi,\omega) &\triangleq \mathcal{F}_3(\Omega_n, \overline{\gamma}_n, -\infty, +\infty, \varphi, \omega).
\end{aligned} \tag{17}$$

Using $\mathcal{H}_1$, we can write the average BER for the FU as

$$\overline{P_{1,2}(e)} = \mathcal{H}_1(\overline{\gamma_{1,A}}). \tag{18}$$

Hence, the average BER is calculated as a function of $\overline{\gamma_{1,A}}$.

2) NU BIT ERROR RATE

For NU to successfully detect its own signal, it must first perform the SIC process, which requires error-free interference cancellation. In other words, if the SIC process has errors, this may cause error propagation to NU detection. The BER for the NU can be computed by considering the two cases of correct SIC and incorrect SIC in the following form:

$$\begin{aligned}
P_{1,1}(e) &= \Pr(\textit{correct SIC})P_{1,1}(e|\textit{correct SIC}) \\
&\quad + \Pr(\textit{incorrect SIC})P_{1,1}(e|\textit{incorrect SIC})
\end{aligned} \tag{19}$$

where the first term on the right-hand side of (19) indicates ideal SIC and the second term is related to the non-ideal case. The required condition for having correct SIC can be stated as

$$n_I \leq \sqrt{\varepsilon_2}|h_1|. \tag{20}$$

Therefore, we can write the first term as

$$\begin{aligned}
&\Pr(\textit{correct SIC})P_{1,1}(e|\textit{correct SIC}) \\
&= \Pr\left(n_I \leq \sqrt{\varepsilon_2}|h_1|\right) \times \Pr\left(n_Q \geq \sqrt{\varepsilon_1}|h_1| \,|\, n_I \leq \sqrt{\varepsilon_2}|h_1|\right) \\
&= \Pr\left(n_I \leq \sqrt{\varepsilon_2}|h_1|\right) \times \Pr\left(n_Q \geq \sqrt{\varepsilon_1}|h_1|\right).
\end{aligned} \tag{21}$$

For this case, we can define the following SNR variables:

$$\begin{aligned}
\gamma_{1,B} &= \frac{2\varepsilon_2|h_1|^2}{N_0}, \quad \overline{\gamma_{1,B}} = \frac{2\varepsilon_2}{N_0}E\{|h_1|^2\}, \\
\gamma_{1,C} &= \frac{2\varepsilon_1|h_1|^2}{N_0}, \quad \overline{\gamma_{1,C}} = \frac{2\varepsilon_1}{N_0}E\{|h_1|^2\}.
\end{aligned} \tag{22}$$

Considering these definitions, the first term on the right-hand side of (19) can be expressed as

$$\begin{aligned}
&\Pr(\textit{correct SIC})P_{1,1}(e|\textit{correct SIC}) \\
&= \left[1 - Q\left(\sqrt{\gamma_{1,B}}\right)\right] \times Q\left(\sqrt{\gamma_{1,C}}\right).
\end{aligned} \tag{23}$$

For the case that error occurs, the required condition is

$$n_I \geq \sqrt{\varepsilon_2}|h_1|. \tag{24}$$

Therefore, the related term can be written as

$$\begin{aligned}
&\Pr(\textit{incorrect SIC})P_{1,1}(e|\textit{incorrect SIC}) \\
&= \Pr\left(n_I \geq \sqrt{\varepsilon_2}|h_1|\right) \times \Pr\left(n_Q \geq \sqrt{\varepsilon_1}|h_1| \,|\, n_I \geq \sqrt{\varepsilon_2}|h_1|\right) \\
&= \Pr\left(n_I \geq \sqrt{\varepsilon_2}|h_1|\right) \times \Pr\left(n_Q \geq \sqrt{\varepsilon_1}|h_1|\right).
\end{aligned} \tag{25}$$

Using $\gamma_{1,B}$ and $\gamma_{1,C}$, we can rewrite (25) as

$$\begin{aligned}
&\Pr(\textit{incorrect SIC})P_{1,1}(e|\textit{incorrect SIC}) \\
&= \mathrm{Q}\left(\sqrt{\gamma_{1,B}}\right)\mathrm{Q}\left(\sqrt{\gamma_{1,C}}\right).
\end{aligned} \tag{26}$$

Substituting (23) and (26) into (19), the BER for the NU can be expressed as

$$\begin{aligned}
P_{1,1}(e) &= \left[1 - \mathrm{Q}\left(\sqrt{\gamma_{1,B}}\right)\right] \times \mathrm{Q}\left(\sqrt{\gamma_{1,C}}\right) + \mathrm{Q}\left(\sqrt{\gamma_{1,B}}\right) \\
&\quad \times \mathrm{Q}\left(\sqrt{\gamma_{1,C}}\right) = \mathrm{Q}\left(\sqrt{\gamma_{1,C}}\right).
\end{aligned} \tag{27}$$

The average BER can be calculated by considering the following integration:

$$\overline{P_{1,1}(e)} = \int_0^\infty \mathrm{Q}\left(\sqrt{\gamma_{1,C}}\right) f_{\gamma_{1,C}}(\gamma_{1,C}) d\gamma_{1,C} \tag{28}$$

Following similar steps to those used for deriving (18), we can express the closed-form average BER for NU as

$$\overline{P_{1,1}(e)} = \mathcal{H}_1\left(\overline{\gamma_{1,C}}\right). \tag{29}$$

B. SECOND SYSTEM MODE ($M_1 = 4$, $M_2 = 2$)

As the second case, we investigate another modulation combination for users. Here, the modulation index for NU is $M_1 = 4$ and for FU is $M_2 = 2$. In this case, the transmitted bits are in the form $\{i_{1,1}i_{1,2}, i_2\}$, as shown in Figure 4. The detection threshold for FU is the axis I and for NU is both I and Q. The constellation for this case is shown in Figure 4.

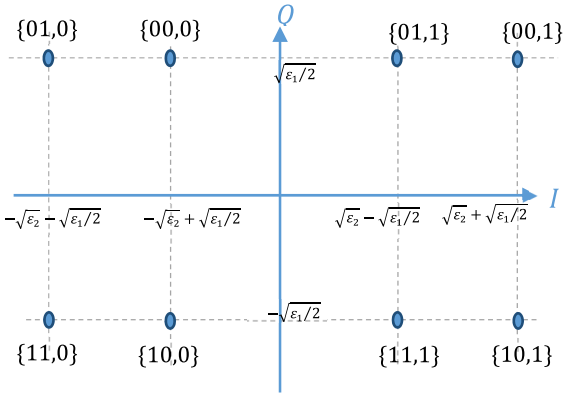

FIGURE 4. Second system mode constellation.

In [12], the BER analysis for this Mode is presented. However, the system is not adaptive, and other modulation combinations for NU and FU were not investigated. The presented derivations in [12] are for a QAM system and the constellation sizes are $M_1 = 2$ and $M_2 = 4$ respectively. For completeness and readability, we also provide the calculations for this scenario.

1) FU BIT ERROR RATE

Error occurs at FU if the following conditions for the symbols are met,

$$n_I \geq \left(\sqrt{\varepsilon_2} + \sqrt{\varepsilon_1/2}\right)|h_2|,\ n_I \geq \left(\sqrt{\varepsilon_2} - \sqrt{\varepsilon_1/2}\right)|h_2|. \tag{30}$$

Like in [12] and by assuming equal priori probability for the symbols, $P_{2,2}(e)$ can be expressed as

$$P_{2,2}(e) = \frac{1}{2}\Big[\Pr\left(n_I \geq \left(\sqrt{\varepsilon_2} + \sqrt{\varepsilon_1/2}\right)|h_2|\right) + \Pr\left(n_I \geq \left(\sqrt{\varepsilon_2} - \sqrt{\varepsilon_1/2}\right)|h_2|\right)\Big] \tag{31}$$

which simplifies to

$$P_{2,2}(e) = \frac{1}{2}\left[\mathrm{Q}\left(\frac{\left(\sqrt{\varepsilon_2} + \sqrt{\varepsilon_1/2}\right)|h_2|}{\sqrt{N_0/2}}\right) + \mathrm{Q}\left(\frac{\left(\sqrt{\varepsilon_2} - \sqrt{\varepsilon_1/2}\right)|h_2|}{\sqrt{N_0/2}}\right)\right]. \tag{32}$$

For this case, we define the following SNR variables:

$$\begin{aligned}
\gamma_{2,A} &= \frac{\left(\sqrt{2\varepsilon_2} + \sqrt{\varepsilon_1}\right)^2 |h_2|^2}{N_0}, \\
\overline{\gamma_{2,A}} &= \frac{\left(\sqrt{2\varepsilon_2} + \sqrt{\varepsilon_1}\right)^2}{N_0} E\left\{|h_2|^2\right\}, \\
\gamma_{2,B} &= \frac{\left(\sqrt{2\varepsilon_2} - \sqrt{\varepsilon_1}\right)^2 |h_2|^2}{N_0}, \\
\overline{\gamma_{2,B}} &= \frac{\left(\sqrt{2\varepsilon_2} - \sqrt{\varepsilon_1}\right)^2}{N_0} E\left\{|h_2|^2\right\}.
\end{aligned} \tag{33}$$

Using these variables, the BER can be expressed as

$$P_{2,2}(e) = \frac{1}{2}\left[\mathrm{Q}\left(\sqrt{\gamma_{2,A}}\right) + \mathrm{Q}\left(\sqrt{\gamma_{2,B}}\right)\right]. \tag{34}$$

By averaging (34) over $\gamma_{2,A}$ and $\gamma_{2,B}$, the average BER for FU can be calculated as

$$\overline{P_{2,2}(e)} = \frac{1}{2}\left[\int_0^\infty \mathrm{Q}\left(\sqrt{\gamma_{2,A}}\right) f_{\gamma_{2,A}}(\gamma_{2,A}) d\gamma_{2,A} + \int_0^\infty \mathrm{Q}\left(\sqrt{\gamma_{2,B}}\right) f_{\gamma_{2,B}}(\gamma_{2,B}) d\gamma_{2,B}\right] \tag{35}$$

which can be expressed in closed-form as

$$\overline{P_{2,2}(e)} = \frac{1}{4}\left[\mathcal{H}_1\left(\overline{\gamma_{2,A}}\right) + \mathcal{H}_1\left(\overline{\gamma_{2,B}}\right)\right]. \tag{36}$$

As it can be seen, the closed-form average BER is formulated as a function of $\overline{\gamma_{2,A}}$ and $\overline{\gamma_{2,B}}$.

2) NU BIT ERROR RATE

The NU must first perform the SIC process which includes detecting and regenerating the FU's signal with 2-QAM modulation. For the NU, the BER is greatly influenced by the SIC process. Based on whether the SIC is ideal or non-ideal, we can compute the BER and combine the results using the following relation:

$$\begin{aligned}
P_{2,1}(e) = {} & \Pr(\textit{correct SIC}) P_{2,1}(e|\textit{correct SIC}) \\
& + \Pr(\textit{incorrect SIC}) P_{2,1}(e|\textit{incorrect SIC})
\end{aligned} \tag{37}$$

where the first term stands for the SIC without errors and the second term is for the unsuccessful SIC. To have a correct SIC, it is required that for the symbols we have

$$n_I \leq \left(\sqrt{\varepsilon_2} + \sqrt{\varepsilon_1/2}\right)|h_1|,\ n_I \leq \left(\sqrt{\varepsilon_2} - \sqrt{\varepsilon_1/2}\right)|h_1|. \tag{38}$$

Therefore, the first term of the right-hand side of (37) can be written as

$$\begin{aligned}
& \Pr(\textit{correct SIC}) P_{2,1}(e|\textit{correct SIC}) \\
& = \frac{1}{2}\Pr\left(n_I \leq \left(\sqrt{\varepsilon_2} - \sqrt{\varepsilon_1/2}\right)|h_1|\right) \\
& \quad \Big\{\Pr\left(n_I \leq -\sqrt{\varepsilon_1/2}|h_1| \,|\, n_I \leq \left(\sqrt{\varepsilon_2} - \sqrt{\varepsilon_1/2}\right)|h_1|\right)
\end{aligned}$$

$$+\Pr\left(n_Q \geq \sqrt{\varepsilon_1/2}|h_1| \,|\, n_I \leq \left(\sqrt{\varepsilon_2}-\sqrt{\varepsilon_1/2}\right)|h_1|\right)\Big\}$$
$$+\frac{1}{2}\Pr\left(n_I \leq \left(\sqrt{\varepsilon_2}+\sqrt{\varepsilon_1/2}\right)|h_1|\right)$$
$$\Big\{\Pr\left(n_I \geq \sqrt{\varepsilon_1/2}|h_1| \,|\, n_I \leq \left(\sqrt{\varepsilon_2}+\sqrt{\varepsilon_1/2}\right)|h_1|\right)$$
$$+\Pr\left(n_Q \geq \sqrt{\varepsilon_1/2}|h_1| \,|\, n_I \leq \left(\sqrt{\varepsilon_2}+\sqrt{\varepsilon_1/2}\right)|h_1|\right)\Big\}. \tag{39}$$

Noting the fact that

$$P(A \,|\, B) = \frac{P(A \cap B)}{P(B)} \tag{40}$$

the right-hand side of (39) can be rewritten as

$$\Pr(\textit{correct SIC})P_{2,1}(e|\textit{correct SIC})$$
$$= \frac{1}{2}\Big[\Pr\left(n_I \leq -\sqrt{\varepsilon_1/2}|h_1|\right) + \Pr\left(\sqrt{\varepsilon_1/2}|h_1| \leq n_I \leq \left(\sqrt{\varepsilon_2}-\sqrt{\varepsilon_1/2}\right)|h_1|\right) + \Pr\left(n_Q \geq \sqrt{\varepsilon_1/2}|h_1|\right)$$
$$\times\Big[\Pr\left(n_I \leq \left(\sqrt{\varepsilon_2}-\sqrt{\varepsilon_1/2}\right)|h_1|\right) + \Pr\left(n_I \leq \left(\sqrt{\varepsilon_2}+\sqrt{\varepsilon_1/2}\right)|h_1|\right)\Big]\Big]. \tag{41}$$

Let us define

$$\gamma_{2,C} = \frac{\varepsilon_1|h_1|^2}{N_0},\ \overline{\gamma_{2,C}} = \frac{\varepsilon_1}{N_0}E\{|h_1|^2\},$$
$$\gamma_{2,E} = \frac{\left(\sqrt{2\varepsilon_2}+\sqrt{\varepsilon_1}\right)^2|h_1|^2}{N_0},$$
$$\overline{\gamma_{2,E}} = \frac{\left(\sqrt{2\varepsilon_2}+\sqrt{\varepsilon_1}\right)^2}{N_0}E\{|h_1|^2\},$$
$$\gamma_{2,D} = \frac{\left(\sqrt{2\varepsilon_2}-\sqrt{\varepsilon_1}\right)^2|h_1|^2}{N_0},$$
$$\overline{\gamma_{2,D}} = \frac{\left(\sqrt{2\varepsilon_2}-\sqrt{\varepsilon_1}\right)^2}{N_0}E\{|h_1|^2\}. \tag{42}$$

According to these definitions, (41) can be presented as

$$\Pr(\textit{correct SIC})P_{2,1}(e|\textit{correct SIC})$$
$$=\frac{1}{4}\left[\mathrm{Q}\left(\sqrt{\gamma_{2,C}}\right)\times\left\{4-\mathrm{Q}\left(\sqrt{\gamma_{2,D}}\right)-\mathrm{Q}\left(\sqrt{\gamma_{2,E}}\right)\right\}-\mathrm{Q}\left(\sqrt{\gamma_{2,D}}\right)\right]. \tag{43}$$

For the second term in the right-hand side of (37), we should first determine the event of incorrect SIC. The incorrect SIC occurs when the NU detects the FU signal erroneously. This situation occurs in the following cases:

$$n_I \geq \left(\sqrt{\varepsilon_2}+\sqrt{\varepsilon_1/2}\right)|h_1|,\ n_I \geq \left(\sqrt{\varepsilon_2}-\sqrt{\varepsilon_1/2}\right)|h_1|. \tag{44}$$

Therefore, the second term in the right-hand side of (37) can be computed as

$$\Pr(\textit{incorrect SIC})P_{2,1}(e|\textit{incorrect SIC})$$
$$=\frac{1}{2}\Pr\left(n_I \geq \left(\sqrt{\varepsilon_2}-\sqrt{\varepsilon_1/2}\right)|h_1|\right)$$
$$\times\Big[\Pr\left(n_I \leq \left(2\sqrt{\varepsilon_2}-\sqrt{\varepsilon_1/2}\right)|h_1| \,|\, n_I \geq \left(\sqrt{\varepsilon_2}-\sqrt{\varepsilon_1/2}\right)|h_1|\right)$$
$$+\Pr\left(n_Q \geq \sqrt{\varepsilon_1}/2|h_1| \,|\, n_I \geq \left(\sqrt{\varepsilon_2}-\sqrt{\varepsilon_1/2}\right)|h_1|\right)\Big]$$
$$+\frac{1}{2}\Pr\left(n_I \geq \left(\sqrt{\varepsilon_2}+\sqrt{\varepsilon_1/2}\right)|h_1|\right)$$
$$\times\Big[\Pr\left(n_I \leq \left(2\sqrt{\varepsilon_2}+\sqrt{\varepsilon_1/2}\right)|h_1| \,|\, n_I \geq \left(\sqrt{\varepsilon_2}+\sqrt{\varepsilon_1/2}\right)|h_1|\right)$$
$$+\Pr\left(n_Q \geq \sqrt{\varepsilon_1/2}|h_1| \,|\, n_I \geq \left(\sqrt{\varepsilon_2}+\sqrt{\varepsilon_1/2}\right)|h_1|\right)\Big]. \tag{45}$$

After simplification, we have

$$\Pr(\textit{incorrect SIC})P_{2,1}(e|\textit{incorrect SIC})$$
$$= \frac{1}{2}\Big[\Pr\left(\left(\sqrt{\varepsilon_2}-\sqrt{\varepsilon_1/2}\right)|h_2| \leq n_I \leq \left(2\sqrt{\varepsilon_2}-\sqrt{\varepsilon_1/2}\right)|h_1|\right)$$
$$+\Pr\left(n_I \geq \left(2\sqrt{\varepsilon_2}+\sqrt{\varepsilon_1/2}\right)|h_1|\right) + \Pr\left(n_Q \geq \sqrt{\varepsilon_1/2}|h_1|\right)$$
$$\times\Big[\Pr\left(n_I \geq \left(\sqrt{\varepsilon_2}-\sqrt{\varepsilon_1/2}\right)|h_1|\right) + \Pr\left(n_I \geq \left(\sqrt{\varepsilon_2}+\sqrt{\varepsilon_1/2}\right)|h_1|\right)\Big]\Big]. \tag{46}$$

Similarly, we define the following SNR variables:

$$\gamma_{2,F} = \frac{\left(2\sqrt{2\varepsilon_2}+\sqrt{\varepsilon_1}\right)^2|h_1|^2}{N_0},$$
$$\overline{\gamma_{2,F}} = \frac{\left(2\sqrt{2\varepsilon_2}+\sqrt{\varepsilon_1}\right)^2}{N_0}E\{|h_1|^2\},$$
$$\gamma_{2,G} = \frac{\left(2\sqrt{2\varepsilon_2}-\sqrt{\varepsilon_1}\right)^2|h_1|^2}{N_0},$$
$$\overline{\gamma_{2,G}} = \frac{\left(2\sqrt{2\varepsilon_2}-\sqrt{\varepsilon_1}\right)^2}{N_0}E\{|h_1|^2\}. \tag{47}$$

Having these definitions, (46) can be rewritten as

$$\Pr(\textit{incorrect SIC})P_{2,1}(e|\textit{incorrect SIC})$$
$$=\frac{1}{4}\left[Q\left(\sqrt{\gamma_{2,C}}\right)\times\left[Q\left(\sqrt{\gamma_{2,D}}\right)+Q\left(\sqrt{\gamma_{2,E}}\right)\right]+Q\left(\sqrt{\gamma_{2,E}}\right)+Q\left(\sqrt{\gamma_{2,F}}\right)-Q\left(\sqrt{\gamma_{2,G}}\right)\right]. \tag{48}$$

Substituting (43) and (48) into (37), we obtain $P_{2,1}(e)$ as

$$P_{2,1}(e) = Q\left(\sqrt{\gamma_{2,C}}\right)+\frac{1}{4}\left[Q\left(\sqrt{\gamma_{2,E}}\right)+Q\left(\sqrt{\gamma_{2,F}}\right)-Q\left(\sqrt{\gamma_{2,G}}\right)-Q\left(\sqrt{\gamma_{2,D}}\right)\right]. \tag{49}$$

Averaging (49) over $\gamma_{2,C}$, $\gamma_{2,E}$, $\gamma_{2,F}$, $\gamma_{2,G}$ and $\gamma_{2,D}$, the average BER for the NU can be calculated as

$$\overline{P_{2,1}(e)} = \int_0^\infty \mathrm{Q}\left(\sqrt{\gamma_{2,C}}\right)f_{\gamma_{2,C}}(\gamma_{2,C})d\gamma_{2,C}$$
$$+\frac{1}{4}\Bigg[\int_0^\infty \mathrm{Q}\left(\sqrt{\gamma_{2,E}}\right)f_{\gamma_{2,E}}(\gamma_{2,E})d\gamma_{2,E}$$
$$+\int_0^\infty \mathrm{Q}\left(\sqrt{\gamma_{2,F}}\right)f_{\gamma_{2,F}}(\gamma_{2,F})d\gamma_{2,F}$$
$$-\int_0^\infty \mathrm{Q}\left(\sqrt{\gamma_{2,G}}\right)f_{\gamma_{2,G}}(\gamma_{2,G})d\gamma_{2,G}$$
$$-\int_0^\infty \mathrm{Q}\left(\sqrt{\gamma_{2,D}}\right)f_{\gamma_{2,D}}(\gamma_{2,D})d\gamma_{2,D}\Bigg]. \tag{50}$$

Following similar steps to those used for deriving the average BER for FU, (54) can be expressed in closed-form as

$$\overline{P_{2,1}(e)} = \mathcal{H}_1\left(\overline{\gamma_{2,C}}\right)+\frac{1}{4}\left[\mathcal{H}_1\left(\overline{\gamma_{2,\mathrm{E}}}\right)+\mathcal{H}_1\left(\overline{\gamma_{2,\mathrm{F}}}\right)-\mathcal{H}_1\left(\overline{\gamma_{2,G}}\right)-\mathcal{H}_1\left(\overline{\gamma_{2,\mathrm{D}}}\right)\right]. \tag{51}$$

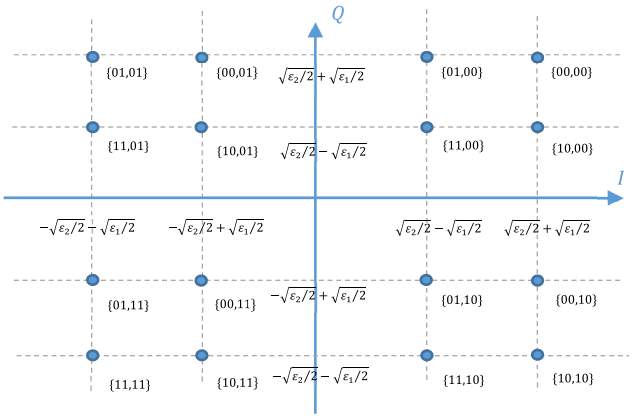

FIGURE 5. Third system mode constellation.

C. THIRD SYSTEM MODE ($M_1 = 4, M_2 = 4$)

The last case stands for the combination of two 4-QAM modulations, i.e., $M_1 = 4$ and $M_2 = 4$. Therefore, the format of the transmitted symbols is $\{i_{1,1}i_{1,2}, i_{2,1}i_{2,2}\}$. In this case, the detection thresholds for both cases are I-axis and Q-axis. Figure 5 illustrates the superimposed signals of both users.

1) FU BIT ERROR RATE

For the FU, the receiver considers the received signal as a 4-QAM constellation and performs detection. In this case, an error occurs if the following event takes place:

$$n_I \geq \sqrt{\varepsilon_2/2}|h_2|+\sqrt{\varepsilon_1/2}|h_2|,\ n_I \geq \sqrt{\varepsilon_2/2}|h_2|-\sqrt{\varepsilon_1/2}|h_2|,$$
$$n_Q \geq \sqrt{\varepsilon_2/2}|h_2|+\sqrt{\varepsilon_1/2}|h_2|,\ n_Q \geq \sqrt{\varepsilon_2/2}|h_2|-\sqrt{\varepsilon_1/2}|h_2|. \tag{52}$$

Therefore, the related BER for this user can be calculated as

$$\begin{aligned} P_{3,2}(e) = \frac{1}{4}\big[&\Pr(n_I \geq \sqrt{\varepsilon_2/2}|h_2| + \sqrt{\varepsilon_1/2}|h_2|) \\ &+ \Pr(n_I \geq \sqrt{\varepsilon_2/2}|h_2| - \sqrt{\varepsilon_1/2}|h_2|) \\ &+ \Pr(n_Q \geq \sqrt{\varepsilon_2/2}|h_2| + \sqrt{\varepsilon_1/2}|h_2|) \\ &+ \Pr(n_Q \geq \sqrt{\varepsilon_2/2}|h_2| - \sqrt{\varepsilon_1/2}|h_2|)\big]. \end{aligned} \tag{53}$$

We know that the in-phase part of the noise affects this probability, hence, according to the noise distribution, we get

$$P_{3,2}(e) = \frac{1}{2}\left[\mathrm{Q}\left(\frac{\sqrt{\varepsilon_2}|h_2|+\sqrt{\varepsilon_1}|h_2|}{\sqrt{N_0}}\right)+\mathrm{Q}\left(\frac{\sqrt{\varepsilon_2}|h_2|-\sqrt{\varepsilon_1}|h_2|}{\sqrt{N_0}}\right)\right]. \tag{54}$$

By defining the following SNR variables:

$$\gamma_{3,A} = \frac{\left(\sqrt{\varepsilon_2}+\sqrt{\varepsilon_1}\right)^2|h_2|^2}{N_0},\ \overline{\gamma_{3,A}} = \frac{\left(\sqrt{\varepsilon_2}+\sqrt{\varepsilon_1}\right)^2}{N_0}E\{|h_2|^2\},$$
$$\gamma_{3,B} = \frac{\left(\sqrt{\varepsilon_2}-\sqrt{\varepsilon_1}\right)^2|h_2|^2}{N_0},\ \overline{\gamma_{3,B}} = \frac{\left(\sqrt{\varepsilon_2}-\sqrt{\varepsilon_1}\right)^2}{N_0}E\{|h_2|^2\} \tag{55}$$

the BER can be expressed as

$$P_{3,2}(e) = \frac{1}{2}\left[\mathrm{Q}\left(\sqrt{\gamma_{3,A}}\right) + \mathrm{Q}\left(\sqrt{\gamma_{3,B}}\right)\right]. \tag{56}$$

By averaging (56) over $\gamma_{3,A}$ and $\gamma_{3,B}$, the average BER can be calculated as

$$\begin{aligned} \overline{P_{3,2}(e)} = \frac{1}{2}\Bigg[&\int_0^\infty \mathrm{Q}\left(\sqrt{\gamma_{3,A}}\right) f_{\gamma_{3,A}}(\gamma_{3,A}) d\gamma_{2,A} \\ &+ \int_0^\infty \mathrm{Q}\left(\sqrt{\gamma_{3,B}}\right) f_{\gamma_{3,B}}(\gamma_{3,B}) d\gamma_{3,B}\Bigg] \end{aligned} \tag{57}$$

which can be expressed in closed-form as

$$\overline{P_{3,2}(e)} = \frac{1}{2}\left[\mathcal{H}_1\left(\overline{\gamma_{3,A}}\right) + \mathcal{H}_1\left(\overline{\gamma_{3,B}}\right)\right]. \tag{58}$$

2) NU BIT ERROR RATE

In order to calculate the BER for the NU, we should consider two possibilities for the SIC, namely, correct SIC and incorrect SIC:

$$\begin{aligned} P_{3,1}(e) = &\Pr(\textit{correct SIC}) P_{3,1}(e|\textit{correct SIC}) \\ &+ \Pr(\textit{incorrect SIC}) P_{3,1}(e|\textit{incorrect SIC}) \end{aligned} \tag{59}$$

where the first term on the right-hand side states the case when the SIC process is correct and the second one stands for incorrect SIC. In order to guarantee correct SIC, there must be

$$n_I \leq \sqrt{\varepsilon_2/2}|h_1|+\sqrt{\varepsilon_1/2}|h_1|,\ n_I \leq \sqrt{\varepsilon_2/2}|h_1|-\sqrt{\varepsilon_1/2}|h_1|,$$
$$n_Q \leq \sqrt{\varepsilon_2/2}|h_1|+\sqrt{\varepsilon_1/2}|h_1|,\ n_Q \leq \sqrt{\varepsilon_2/2}|h_1|-\sqrt{\varepsilon_1/2}|h_1|. \tag{60}$$

According to these inequalities we can calculate the first term in the right-hand side of (59) as

$$\begin{aligned} &\Pr(\textit{correct SIC}) P_{3,1}(e|\textit{correct SIC}) \\ &= \frac{1}{4}\Pr(n_I \leq \sqrt{\varepsilon_2/2}|h_1| - \sqrt{\varepsilon_1/2}|h_1|) \\ &\quad \times \big\{\Pr(n_I \leq -\sqrt{\varepsilon_1/2}|h_1| \,|\, n_I \leq \sqrt{\varepsilon_2/2}|h_1| - \sqrt{\varepsilon_1/2}|h_1|) \\ &\quad + \Pr\left(n_Q \geq \sqrt{\varepsilon_1/2}|h_1| \,|\, n_I \leq \sqrt{\varepsilon_2/2}|h_1| - \sqrt{\varepsilon_1/2}|h_1|\right)\big\} \\ &\quad + \frac{1}{4}\Pr(n_I \leq \sqrt{\varepsilon_2/2}|h_1| + \sqrt{\varepsilon_1/2}|h_1|) \\ &\quad \times \big\{\Pr(n_I \geq \sqrt{\varepsilon_1/2}h_1 \,|\, n_I \leq \sqrt{\varepsilon_2/2}|h_1| + \sqrt{\varepsilon_1/2}|h_1|) \\ &\quad + \Pr(n_Q \geq \sqrt{\varepsilon_1/2}h_1 \,|\, n_I \leq \sqrt{\varepsilon_2/2}|h_1| + \sqrt{\varepsilon_1/2}|h_1|)\big\} \\ &\quad + \frac{1}{4}\Pr(n_Q \leq \sqrt{\varepsilon_2/2}|h_1| - \sqrt{\varepsilon_1/2}|h_1|) \\ &\quad \times \big\{\Pr(n_I \geq \sqrt{\varepsilon_1/2}|h_1| \,|\, n_Q \leq \sqrt{\varepsilon_2/2}|h_1| - \sqrt{\varepsilon_1/2}|h_1|) \\ &\quad + \Pr\left(n_Q \leq -\sqrt{\varepsilon_1/2}|h_1| \,|\, n_Q \leq \sqrt{\varepsilon_2/2}|h_1| - \sqrt{\varepsilon_1/2}|h_1|\right)\big\} \\ &\quad + \frac{1}{4}\Pr(n_Q \leq \sqrt{\varepsilon_2/2}|h_1| + \sqrt{\varepsilon_1/2}|h_1|) \\ &\quad \times \big\{\Pr(n_I \geq \sqrt{\varepsilon_1/2}|h_1| \,|\, n_Q \leq \sqrt{\varepsilon_2/2}|h_2| + \sqrt{\varepsilon_1/2}|h_1|) \\ &\quad + \Pr(n_Q \geq \sqrt{\varepsilon_1/2}|h_1| \,|\, n_Q \leq \sqrt{\varepsilon_2/2}|h_2| + \sqrt{\varepsilon_1/2}|h_1|)\big\}. \end{aligned} \tag{61}$$

According to the conditional probability relation, after some manipulations, we have

$$\begin{aligned}
&\Pr(\textit{correct SIC})P_{3,1}(e|\textit{correct SIC})\\
&=\frac{1}{4}\big[\Pr(n_I\le-\sqrt{\varepsilon_1/2}|h_1|)+\Pr(n_Q\ge\sqrt{\varepsilon_1/2}|h_1|)\\
&\quad\times\Pr(n_I\le\sqrt{\varepsilon_2/2}|h_1|-\sqrt{\varepsilon_1/2}|h_1|)+\Pr(\sqrt{\varepsilon_1/2}|h_1|\\
&\le n_I\le\sqrt{\varepsilon_2/2}|h_1|+\sqrt{\varepsilon_1/2}|h_1|)+\Pr(n_Q\ge\sqrt{\varepsilon_1/2}|h_1|)\\
&\quad\times\Pr(n_I\le\sqrt{\varepsilon_2/2}|h_1|+\sqrt{\varepsilon_1/2}|h_1|)+\Pr(n_Q\le\sqrt{\varepsilon_2/2}|h_1|\\
&\quad-\sqrt{\varepsilon_1/2}|h_1|)\Pr(n_I\ge\sqrt{\varepsilon_1/2}|h_1|)+\Pr(n_Q\le-\sqrt{\varepsilon_1/2}|h_1|)\\
&\quad+\Pr(n_Q\le\sqrt{\varepsilon_2/2}|h_1|+\sqrt{\varepsilon_1/2}|h_1|)\Pr(n_I\ge\sqrt{\varepsilon_1/2}|h_1|)\\
&\quad+\Pr(\sqrt{\varepsilon_1/2}|h_1|\le n_Q\le\sqrt{\varepsilon_2/2}|h_1|+\sqrt{\varepsilon_1/2}|h_1|)\big].
\end{aligned}\tag{62}$$

The right-hand side of (62) can be expressed as

$$\begin{aligned}
&\frac{1}{4}\big[\Pr(n_I\ge\sqrt{\varepsilon_1/2}|h_1|)\{1+\Pr(n_Q\le\sqrt{\varepsilon_2/2}|h_1|\\
&\quad-\sqrt{\varepsilon_1/2}|h_1|)+\Pr(n_Q\le\sqrt{\varepsilon_2/2}|h_1|+\sqrt{\varepsilon_1/2}|h_1|)\}\\
&\quad+\Pr(n_Q\ge\sqrt{\varepsilon_1/2}|h_1|)\{1+\Pr(n_I\le\sqrt{\varepsilon_2/2}|h_1|\\
&\quad-\sqrt{\varepsilon_1/2}|h_1|)+\Pr(n_I\le\sqrt{\varepsilon_2/2}|h_1|+\sqrt{\varepsilon_1/2}|h_1|)\}\\
&\quad+\Pr(\sqrt{\varepsilon_1/2}|h_1|\le n_Q\le\sqrt{\varepsilon_2/2}|h_1|+\sqrt{\varepsilon_1/2}|h_1|)\\
&\quad+\Pr(\sqrt{\varepsilon_1/2}|h_1|\le n_I\le\sqrt{\varepsilon_2/2}|h_1|+\sqrt{\varepsilon_1/2}|h_1|)\big].
\end{aligned}\tag{63}$$

For this case, we can define the corresponding SNR as

$$\begin{aligned}
&\gamma_{3,C}=\frac{\left(\sqrt{\varepsilon}_2+\sqrt{\varepsilon}_1\right)^2|h_1|^2}{N_0},\overline{\gamma_{3,C}}=\frac{\left(\sqrt{\varepsilon}_2+\sqrt{\varepsilon}_1\right)^2}{N_0}E\{|h_1|^2\}\\
&\gamma_{3,D}=\frac{\left(\sqrt{\varepsilon}_2-\sqrt{\varepsilon}_1\right)^2|h_1|^2}{N_0},\ \overline{\gamma_{3,D}}=\frac{\left(\sqrt{\varepsilon}_2-\sqrt{\varepsilon}_1\right)^2}{N_0}E\{|h_1|^2\}\\
&\gamma_{3,E}=\frac{\varepsilon_1|h_1|^2}{N_0},\ \overline{\gamma_{3,E}}=\frac{\varepsilon_1}{N_0}E\{|h_1|^2\}.
\end{aligned}\tag{64}$$

Using these SNRs, we can write

$$\begin{aligned}
P_{3,1}(e|\textit{correct SIC})=\frac{1}{4}\big[&\mathrm{Q}(\sqrt{\gamma_{3,E}})\times\{8-2\mathrm{Q}(\sqrt{\gamma_{3,C}})\\
&-2\mathrm{Q}(\sqrt{\gamma_{3,D}})\}-2\mathrm{Q}(\sqrt{\gamma_{3,C}})\big].
\end{aligned}\tag{65}$$

After calculating the correct SIC, the next step is to calculate the incorrect SIC. For this case, the condition to have erroneous SIC is to have the following conditions

$$\begin{aligned}
&n_I\ge\sqrt{\varepsilon_2/2}|h_1|+\sqrt{\varepsilon_1/2}|h_1|,\ n_I\ge\sqrt{\varepsilon_2/2}|h_1|-\sqrt{\varepsilon_1/2}|h_1|,\\
&n_Q\ge\sqrt{\varepsilon_2/2}|h_1|+\sqrt{\varepsilon_1/2}|h_1|,\ n_Q\ge\sqrt{\varepsilon_2/2}|h_1|-\sqrt{\varepsilon_1/2}|h_1|.
\end{aligned}\tag{66}$$

This can be expressed in terms of conditional probability, which is provided in Appendix A, for simplicity, we express it as

$$\begin{aligned}
&\Pr(\textit{incorrect SIC})P_{3,1}(e|\textit{incorrect SIC})\\
&=\frac{1}{4}\big[\Pr(n_I\ge\sqrt{\varepsilon_2/2}|h_1|-\sqrt{\varepsilon_1/2}|h_1|)\Psi(n_I\ge\sqrt{\varepsilon_2/2}|h_1|\\
&\quad-\sqrt{\varepsilon_1/2}|h_1|)+\Pr(n_I\ge\sqrt{\varepsilon_2/2}|h_1|+\sqrt{\varepsilon_1/2}|h_1|)\Psi(n_I\\
&\quad\ge\sqrt{\varepsilon_2/2}|h_1|+\sqrt{\varepsilon_1/2}|h_1|)+\Pr(n_Q\ge\sqrt{\varepsilon_2/2}|h_1|\\
&\quad-\sqrt{\varepsilon_1/2}|h_1|)\Psi(n_Q\ge\sqrt{\varepsilon_2/2}|h_1|-\sqrt{\varepsilon_1/2}|h_1|)\\
&\quad+\Pr(n_Q\ge\sqrt{\varepsilon_2/2}|h_1|+\sqrt{\varepsilon_1/2}|h_1|)\Psi(n_Q\ge\sqrt{\varepsilon_2/2}|h_1|\\
&\quad+\sqrt{\varepsilon_1/2}|h_1|)\big].
\end{aligned}\tag{67}$$

where we have

$$\begin{aligned}
\Psi(\mathrm{X})=&\Pr(n_I\ge-2\sqrt{\varepsilon_2/2}|h_1|+\sqrt{\varepsilon_1/2}|h_1|\,|\,\mathrm{X})\\
&+\Pr(n_Q\ge-2\sqrt{\varepsilon_2/2}|h_1|+\sqrt{\varepsilon_1/2}|h_1|\,|\,\mathrm{X})\\
&+\Pr(n_I\ge-2\sqrt{\varepsilon_2/2}|h_1|-\sqrt{\varepsilon_1/2}|h_1|\,|\,\mathrm{X})\\
&+\Pr(n_Q\ge-2\sqrt{\varepsilon_2/2}|h_1|-\sqrt{\varepsilon_1/2}|h_1|\,|\,\mathrm{X}).
\end{aligned}\tag{68}$$

According to the conditional probability, we can write $P_{3,1}(e|\textit{incorrect SIC})$ as in Appendix B. For this case, we can define the SNR variables as

$$\begin{aligned}
\gamma_{3,F}&=\frac{\left(2\sqrt{\varepsilon}_2+\sqrt{\varepsilon}_1\right)^2|h_1|^2}{N_0},\\
\overline{\gamma_{3,F}}&=\frac{\left(2\sqrt{\varepsilon}_2+\sqrt{\varepsilon}_1\right)^2}{N_0}E\{|h_1|^2\},\\
\gamma_{3,G}&=\frac{\left(2\sqrt{\varepsilon}_2-\sqrt{\varepsilon}_1\right)^2|h_1|^2}{N_0},\\
\overline{\gamma_{3,G}}&=\frac{\left(2\sqrt{\varepsilon}_2-\sqrt{\varepsilon}_1\right)^2}{N_0}E\{|h_1|^2\}.
\end{aligned}\tag{69}$$

Therefore, the BER for FU can be obtained as

$$\begin{aligned}
&\Pr(\textit{incorrect SIC})P_{3,1}(e|\textit{incorrect SIC})\\
&=\frac{1}{4}[\mathrm{Q}(\sqrt{\gamma_{3,F}})+\mathrm{Q}(\sqrt{\gamma_{3,G}})]\{4-2(\mathrm{Q}(\sqrt{\gamma_{3,C}})+\mathrm{Q}(\sqrt{\gamma_{3,D}}))\}.
\end{aligned}\tag{70}$$

Substituting (65) and (70) into (59), we get

$$\begin{aligned}
P_{3,1}(e)=&\frac{1}{4}\big[\mathrm{Q}(\sqrt{\gamma_{3,E}})\times\{8-2\mathrm{Q}(\sqrt{\gamma_{3,C}})-2\mathrm{Q}(\sqrt{\gamma_{3,D}})\}\\
&-2\mathrm{Q}(\sqrt{\gamma_{3,C}})\big]+\frac{1}{4}[\mathrm{Q}(\sqrt{\gamma_{3,F}})+\mathrm{Q}(\sqrt{\gamma_{3,G}})]\{4\\
&-2(\mathrm{Q}(\sqrt{\gamma_{3,C}})+\mathrm{Q}(\sqrt{\gamma_{3,D}}))\}.
\end{aligned}\tag{71}$$

By averaging (71) over the instantaneous SNRs and using $\mathcal{H}_2$ defined in (17), the average BER can be obtained as

$$\begin{aligned}
\overline{P_{3,1}(e)}=&\frac{1}{2}\big[4\mathcal{H}_1(\overline{\gamma_{3,E}})+\frac{1}{2}\mathcal{H}_2(\overline{\gamma_{3,E}},\overline{\gamma_{3,C}})\\
&-\mathcal{H}_2(\overline{\gamma_{3,E}},\overline{\gamma_{3,D}})-\mathcal{H}_1(\overline{\gamma_{3,C}})+2\mathcal{H}_1(\overline{\gamma_{3,F}})\\
&+2\mathcal{H}_1(\overline{\gamma_{3,G}})-\mathcal{H}_2(\overline{\gamma_{3,F}},\overline{\gamma_{3,C}})-\mathcal{H}_2(\overline{\gamma_{3,F}},\overline{\gamma_{3,D}})\\
&-\mathcal{H}_2(\overline{\gamma_{3,G}},\overline{\gamma_{3,C}})-\mathcal{H}_2(\overline{\gamma_{3,G}},\overline{\gamma_{3,D}})\big].
\end{aligned}\tag{72}$$

We therefore completed the derivation of closed-form expressions for the average BER for all $\overline{P_{i,j}(e)}$, $i=1,..3,j=1$ (i.e. NU), 2 (i.e. FU).

IV. ADAPTIVE MODULATION FOR THROUGHPUT MAXIMIZATION

In this section, we introduce an adaptive modulation scheme where the BS dynamically selects the appropriate modulation orders for NU and FU based on their channel conditions. The main objective of this scheme is to enhance system throughput while maintaining reliable communication. This is accomplished by selecting the modulation orders that maximize the transmission rate while meeting a predetermined limit on the highest permissible BER. This constraint guarantees that the system maintains a balance between throughput performance and error resilience, adapting to varying channel conditions effectively. This can be done by solving an optimization problem which can be formulated as

$$\max_{M_1,M_2} \; nlog_2M_1 + nlog_2M_2$$
$$s.t.\max\big(\mathrm{BER}_1(M_1,M_2),\mathrm{BER}_2(M_1,M_2)\big) \le \mathrm{BER}_{\mathrm{tar}} \quad (73)$$

where BER_1 and BER_2 represent the closed-form BER expressions derived in the previous section for NU and FU, respectively, and BER_{tar} is the maximum acceptable BER for the system. It is worth noting that the objective function of (73) increases when the system Mode changes from 1 to 2 and from 2 to 3. In other words, the objective function is an increasing function of the system Mode. Under these circumstances, the solution of (73) is Mode 3 if this state satisfies the BER constraint. Otherwise, the solution of the problem is Mode 2 provided that this Mode satisfies the BER constraint. If neither Mode 3 nor Mode 2 satisfies the BER constraint, the solution of the problem is Mode 1 given that this Mode meets the BER constraint. Otherwise, (73) is not feasible and the system is in outage state. Let $\gamma_1 = \varepsilon_1|h_1|^2/N_0$ and $\gamma_2 = \varepsilon_2|h_2|^2/N_0$ denote the SNR values for NU and FU, respectively. Figure 6 shows the system Mode as a function of γ_1 and γ_2 for $\mathrm{BER}_{\mathrm{tar}} = 10^{-2}$. In this figure, Mode 0 corresponds to the outage state. As we observe, with increasing SNR, the system Mode increases gradually from 0 to 3.

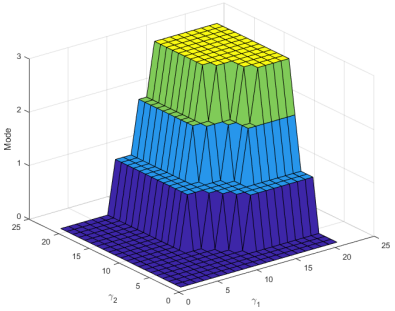

FIGURE 6. 3D mapping for γ_1 and γ_2.

Considering a top view of Figure 6, we obtain Figure 7 as a 2D illustration composed of 4 regions corresponding to 4 system Modes. The colors dark blue, light blue, green and yellow show Modes 0 to 3, respectively. This figure can be re-plotted as Figure 8 by approximating the boundaries with straight lines.

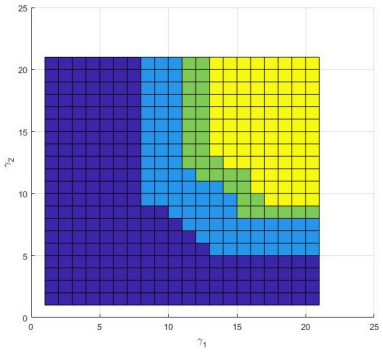

FIGURE 7. 2D display of the mapping.

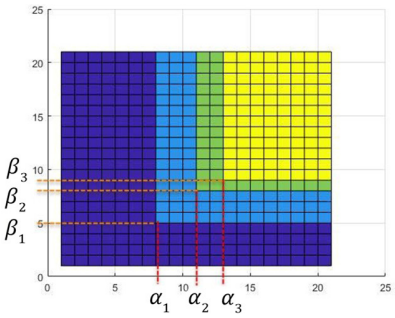

FIGURE 8. Regions for (M_1, M_2) pairs.

The thresholds the three active regions, which are represented as α_i and β_i for $i = 1, 2, 3$, should be calculated next. To this end, we need to consider the BER expressions derived in the previous section and solve the equation $\max(BER_1, BER_2) = BER_{tar}$ to obtain the thresholds for γ_1 and γ_2. To simplify the equation, we can set $\gamma_2 = \infty$ to obtain α_i and set $\gamma_1 = \infty$ to obtain β_i.

After investigating the BER equations, the result for the threshold values can be expressed as in Table 1.

TABLE 1. Threshold values.

Mode	α	β
(2QAM, 2QAM)	$7.8dB$	$4.9dB$
(4QAM, 2QAM)	$11.2dB$	$8.1dB$
(4QAM, 4QAM)	$13.4dB$	$9dB$

As the next step, using the results in section III, we define $\gamma_{i,j}$ as

$$\gamma_{i,j} \triangleq \frac{\left(\mathrm{x}_1\sqrt{\varepsilon}_2 + \mathrm{x}_2\sqrt{\varepsilon}_1\right)^2 |h_{\mathrm{x}_3}|^2}{N_0} \quad (74)$$

where $i = \{1, 2, 3\}, j = \{A, B, C, D, E, F, G\}$.

TABLE 2. $\gamma_{i,j}$ parameters.

variable $\gamma_{i,j}$	x_1	x_2	x_3
$\gamma_{1,A}$	0	$\sqrt{2}$	2
$\gamma_{1,C}$	$\sqrt{2}$	0	1
$\gamma_{2,A}$	1	$\sqrt{2}$	2
$\gamma_{2,B}$	-1	$\sqrt{2}$	2
$\gamma_{2,C}$	1	0	1
$\gamma_{2,E}$	1	$\sqrt{2}$	1
$\gamma_{2,D}$	-1	$\sqrt{2}$	1
$\gamma_{2,F}$	1	$2\sqrt{2}$	1
$\gamma_{2,G}$	-1	$2\sqrt{2}$	1
$\gamma_{3,A}$	1	1	2
$\gamma_{3,B}$	-1	1	2
$\gamma_{3,C}$	1	1	1
$\gamma_{3,D}$	-1	1	1
$\gamma_{3,E}$	1	0	1
$\gamma_{3,F}$	1	2	1
$\gamma_{3,G}$	-1	2	1

Using x_1, x_2, and x_3 from Table 2, all $\gamma_{i,j}$ values can be determined. For example, based on this table, $\gamma_{2,D}$ is given by

$$\gamma_{2,D} = \frac{\left(\sqrt{2\varepsilon_2} - \sqrt{\varepsilon_1}\right)^2 |h_1|^2}{N_0}. \tag{75}$$

Having these values, now we are able to write the BER expressions for different operational Modes. Therefore

$$\mathrm{BER}_1(2,2) = \mathrm{Q}\left(\sqrt{\gamma_{1,C}}\right), \tag{76}$$

$$\mathrm{BER}_1(4,2) = Q\left(\sqrt{\gamma_{2,C}}\right) + \frac{1}{4}\left[Q\left(\sqrt{\gamma_{2,E}}\right) + Q\left(\sqrt{\gamma_{2,F}}\right) - Q\left(\sqrt{\gamma_{2,G}}\right) - Q\left(\sqrt{\gamma_{2,D}}\right)\right], \tag{77}$$

$$\mathrm{BER}_1(4,4) = \frac{1}{4}\left[\mathrm{Q}\left(\sqrt{\gamma_{3,E}}\right) \times \left\{8 - 2\mathrm{Q}\left(\sqrt{\gamma_{3,C}}\right) - 2\mathrm{Q}\left(\sqrt{\gamma_{3,D}}\right)\right\} - 2\mathrm{Q}\left(\sqrt{\gamma_{3,C}}\right)\right] + \frac{1}{4}\left[\mathrm{Q}\left(\sqrt{\gamma_{3,F}}\right) + \mathrm{Q}\left(\sqrt{\gamma_{3,G}}\right)\right] \times \left\{4 - 2\left(\mathrm{Q}\left(\sqrt{\gamma_{3,C}}\right) + \mathrm{Q}\left(\sqrt{\gamma_{3,D}}\right)\right)\right\}, \tag{78}$$

$$\mathrm{BER}_2(2,2) = \mathrm{Q}\left(\sqrt{\gamma_{1,A}}\right), \tag{79}$$

$$\mathrm{BER}_2(4,2) = \frac{1}{2}\left[\mathrm{Q}\left(\sqrt{\gamma_{2,A}}\right) + \mathrm{Q}\left(\sqrt{\gamma_{2,B}}\right)\right], \tag{80}$$

$$\mathrm{BER}_2(4,4) = \frac{1}{2}\left[\mathrm{Q}\left(\sqrt{\gamma_{3,A}}\right) + \mathrm{Q}\left(\sqrt{\gamma_{3,B}}\right)\right]. \tag{81}$$

Having these instantaneous BER expressions, (73) can be solved to find the optimum M_1 and M_2 values i.e. system Mode.

V. PERFORMANCE ANALYSIS

After formulating the problem, in this section, we aim to make a comprehensive analysis of the system in different aspects.

A. THROUGHPUT

As it was discussed for problem formulation, the throughput of the system can be expressed as a closed-form function. Therefore, having the modulation dimension, i.e., (M_1, M_2), and counting the number of bits in error we can calculate the instantaneous throughput of the system. It is worth mentioning that we can also define $T(M_1, M_2)$ as the throughput, which can be expressed as

$$T(M_1, M_2) = \sum_{i=1}^{2} \frac{nlog_2 M_i - EB_i}{nlog_2 M_i}. \tag{82}$$

In Equation (82), n stands for the number of all transmitted symbols and EB represents the number of erroneous bits which refers to the bits that are received with error.

B. AVERAGE BER

By averaging the error rate over all system Modes, we obtain the average BER of the system. Let N^{total} and N^{error} denote the number of all bits and the number of bits in error, respectively. Hence, we can write

$$\mathrm{BER}_{\mathrm{avg}} = \frac{N^{error}}{N^{total}}. \tag{83}$$

N^{error} can be calculated as

$$N^{error} = \sum_{k=1}^{3} \int_0^\infty \int_0^\infty \left(M_{1_k}.log_2 M_{1_k}.\mathrm{BER}\left(M_{1_k}, M_{2_k}\right) + M_{2_k}.log_2 M_{2_k}.\mathrm{BER}\left(M_{1_k}, M_{2_k}\right)\right)\Theta(\gamma_1, \gamma_2, k) \times p(\gamma_1)p(\gamma_2)d\gamma_1 d\gamma_2 \tag{84}$$

where $k = 1, \ldots, 3$ represents the operational Modes of the system presented in Section III, $p(\gamma_1)$ and $p(\gamma_2)$ are the PDFs of γ_1 and γ_2 and the function $\Theta(.)$ is defined as

$$\Theta(\gamma_1, \gamma_2, k) = \begin{cases} 1 & \gamma_1, \gamma_2 \in \mathcal{R}_k \\ 0 & \gamma_1, \gamma_2 \notin \mathcal{R}_k. \end{cases} \tag{85}$$

The above equation means that if γ_1 and γ_2 are in the operational region $\mathcal{R}_k$ (that corresponds to Mode k), then it is equal to 1 and otherwise 0.

We can separate the number of erroneous bits for NU and FU as

$$N^{error} = N_1^{error} + N_2^{error}. \tag{86}$$

Therefore, we can write

$$N_1^{error} = \sum_{k=1}^{3} \int_0^\infty \int_0^\infty M_{1_k}.log_2 M_{1_k}.\mathrm{BER}\left(M_{1_k}, M_{2_k}\right) \Theta(\gamma_1, \gamma_2, k)p(\gamma_1)p(\gamma_2)d\gamma_1 d\gamma_2, \tag{87}$$

$$N_2^{error} = \sum_{k=1}^{3} \int_0^\infty \int_0^\infty M_{2_k}.log_2 M_{2_k}.\mathrm{BER}\left(M_{1_k}, M_{2_k}\right) \Theta(\gamma_1, \gamma_2, k)p(\gamma_1)p(\gamma_2)d\gamma_1 d\gamma_2. \tag{88}$$

To compute N_1^{error}, We can divide the integration domain into two rectangular regions: one oriented vertically and the other

horizontally. In other words, the integral regions R_k can be expressed as

$$\begin{aligned}\mathcal{R}_k &= \mathcal{R}_k^1 \cup R_k^2,\\ \mathcal{R}_k^1 &= \{\alpha_k \le \gamma_1 < \alpha_{k+1}, \beta_k \le \gamma_2 < \infty\},\\ \mathcal{R}_k^2 &= \{\alpha_{k+1} \le \gamma_1 < \infty, \beta_k \le \gamma_2 < \beta_{k+1}\}.\end{aligned} \tag{89}$$

Based on these definitions, N_1^{error} can be calculated as the sum of the integrals over the vertical and horizontal rectangular regions, i.e.

$$\begin{aligned}N_1^{error} = &\sum_{k=1}^{3}\int_{\beta_k}^{\infty}\int_{\alpha_k}^{\alpha_{k+1}} M_{1_k}.log_2 M_{1_k}.\mathrm{BER}_1\left(M_{1_k}, M_{2_k}\right)\\ &\Theta(\gamma_1,\gamma_2,k)p(\gamma_1)p(\gamma_2)d\gamma_1 d\gamma_2\\ &+\sum_{k=1}^{3}\int_{\beta_k}^{\beta_{k+1}}\int_{\alpha_{k+1}}^{\infty} M_{1_k}.log_2 M_{1_k}.\mathrm{BER}_1\left(M_{1_k}, M_{2_k}\right)\\ &\Theta(\gamma_1,\gamma_2,k)p(\gamma_1)p(\gamma_2)d\gamma_1 d\gamma_2.\end{aligned} \tag{90}$$

Similarly, for N_2^{error} we have

$$\begin{aligned}N_2^{error} = &\sum_{k=1}^{3}\int_{\beta_k}^{\infty}\int_{\alpha_k}^{\alpha_{k+1}} M_{2_k}.log_2 M_{2_k}.\mathrm{BER}_2\left(M_{1_k}, M_{2_k}\right)\\ &\Theta(\gamma_1,\gamma_2,k)p(\gamma_1)p(\gamma_2)d\gamma_1 d\gamma_2\\ &+\sum_{k=1}^{3}\int_{\beta_k}^{\beta_{k+1}}\int_{\alpha_{k+1}}^{\infty} M_{2_k}.log_2 M_{2_k}.\mathrm{BER}_2\left(M_{1_k}, M_{2_k}\right)\\ &\Theta(\gamma_1,\gamma_2,k)p(\gamma_1)p(\gamma_2)d\gamma_1 d\gamma_2.\end{aligned} \tag{91}$$

To obtain closed-form expressions for N_1^{error} and N_2^{error}, we need to use the functions $\mathcal{F}$ defined in (16). Let us define $\mathcal{G}_1$ to $\mathcal{G}_4$ as

$$\begin{aligned}\mathcal{G}_1(\varphi) &\triangleq \mathcal{F}_2(\Omega_n, \overline{\gamma}_n, \alpha_k, \alpha_{k+1}, \varphi),\\ \mathcal{G}_2(\varphi,\omega) &\triangleq \mathcal{F}_3(\Omega_n, \overline{\gamma}_n, \alpha_k, \alpha_{k+1}, \varphi, \omega),\\ \mathcal{G}_3(\varphi) &\triangleq \mathcal{F}_2(\Omega_n, \overline{\gamma}_n, \alpha_{k+1}, \infty, \varphi),\\ \mathcal{G}_4(\varphi,\omega) &\triangleq \mathcal{F}_3(\Omega_n, \overline{\gamma}_n, \alpha_{k+1}, \infty, \varphi, \omega).\end{aligned} \tag{92}$$

Therefore, N_1^{error} and N_2^{error} can be obtained as

$$\begin{aligned}N_1^{error} = &\mathcal{F}_1(\Omega_1, \overline{\gamma}_1, \beta_k, \infty)\big[M_{1_1}.log_2 M_{1_1}\left(\mathcal{G}_1\left(\sqrt{\gamma_{1,C}}\right)\right)\\ &+M_{1_2}.log_2 M_{1_2}\left(\mathcal{G}_1\left(\sqrt{\gamma_{2,C}}\right)+\frac{1}{4}\mathcal{G}_1\left(\sqrt{\gamma_{2,E}}\right)\right.\\ &+\frac{1}{4}\mathcal{G}_1\left(\sqrt{\gamma_{2,F}}\right)-\frac{1}{4}\mathcal{G}_1\left(\sqrt{\gamma_{2,G}}\right)-\frac{1}{4}\mathcal{G}_1\left(\sqrt{\gamma_{2,D}}\right)\\ &+\mathcal{G}_1\left(\sqrt{\gamma_{2,C}}\right)+\frac{1}{4}\mathcal{G}_1\left(\sqrt{\gamma_{2,E}}\right)+\frac{1}{4}\mathcal{G}_1\left(\sqrt{\gamma_{2,F}}\right)\\ &\left.-\frac{1}{4}\mathcal{G}_1\left(\sqrt{\gamma_{2,G}}\right)-\frac{1}{4}\mathcal{G}_1\left(\sqrt{\gamma_{2,D}}\right)\right)+M_{1_3}\\ &.log_2 M_{1_3}\left(2G_1\left(\sqrt{\gamma_{3,E}}\right)-\frac{1}{2}G_2\left(\sqrt{\gamma_{3,E}},\sqrt{\gamma_{3,C}}\right)\right.\\ &-\frac{1}{2}G_2\left(\sqrt{\gamma_{3,E}},\sqrt{\gamma_{3,D}}\right)-\frac{1}{2}G_1\left(\sqrt{\gamma_{3,C}}\right)\\ &+G_1\left(\sqrt{\gamma_{3,F}}\right)+G_1\left(\sqrt{\gamma_{3,G}}\right)-\frac{1}{2}\mathcal{G}_2\left(\sqrt{\gamma_{3,F}},\sqrt{\gamma_{3,D}}\right)-\frac{1}{2}\mathcal{G}_2\left(\sqrt{\gamma_{3,G}},\sqrt{\gamma_{3,C}}\right)\\ &\left.-\frac{1}{2}\mathcal{G}_2\left(\sqrt{\gamma_{3,G}},\sqrt{\gamma_{3,D}}\right)\right]+\mathcal{F}_1(\Omega_1,\overline{\gamma}_1,\beta_k,\beta_{k+1})\\ &\times\big[M_{1_1}.log_2 M_{1_1}\left(\mathcal{G}_3\left(\sqrt{\gamma_{1,C}}\right)\right)+M_{1_2}\\ &.log_2 M_{1_2}\left(\mathcal{G}_3\left(\sqrt{\gamma_{2,C}}\right)+\frac{1}{4}\mathcal{G}_3\left(\sqrt{\gamma_{2,E}}\right)\right.\\ &+\frac{1}{4}\mathcal{G}_3\left(\sqrt{\gamma_{2,F}}\right)-\frac{1}{4}\mathcal{G}_3\left(\sqrt{\gamma_{2,G}}\right)-\frac{1}{4}\mathcal{G}_3\left(\sqrt{\gamma_{2,D}}\right)\\ &+\mathcal{G}_3\left(\sqrt{\gamma_{2,C}}\right)+\frac{1}{4}\mathcal{G}_3\left(\sqrt{\gamma_{2,E}}\right)+\frac{1}{4}\mathcal{G}_3\left(\sqrt{\gamma_{2,F}}\right)\\ &\left.-\frac{1}{4}\mathcal{G}_3\left(\sqrt{\gamma_{2,G}}\right)-\frac{1}{4}\mathcal{G}_3\left(\sqrt{\gamma_{2,D}}\right)\right)+M_{1_3}\\ &.log_2 M_{1_3}\left(2G_3\left(\sqrt{\gamma_{3,E}}\right)-\frac{1}{2}G_4\left(\sqrt{\gamma_{3,E}},\sqrt{\gamma_{3,C}}\right)\right.\\ &-\frac{1}{2}G_4\left(\sqrt{\gamma_{3,E}},\sqrt{\gamma_{3,D}}\right)-\frac{1}{2}G_3\left(\sqrt{\gamma_{3,C}}\right)\\ &+G_3\left(\sqrt{\gamma_{3,F}}\right)+G_3\left(\sqrt{\gamma_{3,G}}\right)\\ &-\frac{1}{2}\mathcal{G}_4\left(\sqrt{\gamma_{3,F}},\sqrt{\gamma_{3,C}}\right)-\frac{1}{2}\mathcal{G}_4\left(\sqrt{\gamma_{3,F}},\sqrt{\gamma_{3,D}}\right)\\ &\left.-\frac{1}{2}\mathcal{G}_4\left(\sqrt{\gamma_{3,G}},\sqrt{\gamma_{3,C}}\right)-\frac{1}{2}\mathcal{G}_4\left(\sqrt{\gamma_{3,G}},\sqrt{\gamma_{3,D}}\right)\right)\big].\end{aligned} \tag{93}$$

$$\begin{aligned}N_2^{error} = &\mathcal{F}_1(\Omega_2,\overline{\gamma}_2,\beta_k,\infty)\big[M_{2_1}.log_2 M_{2_1}G_1\left(\sqrt{\gamma_{1,A}}\right)\\ &+\frac{1}{2}M_{2_1}.log_2 M_{2_1}\left(G_1\left(\sqrt{\gamma_{2,A}}\right)+\mathcal{G}_1\left(\sqrt{\gamma_{2,B}}\right)\right)\\ &+\frac{1}{2}M_{3_1}.log_2 M_{3_1}\left(G_1\left(\sqrt{\gamma_{3,A}}\right)+G_1\left(\sqrt{\gamma_{3,B}}\right)\right)\big]\\ &+\mathcal{F}_1(\Omega_2,\overline{\gamma}_2,\beta_k,\beta_{k+1})\big[M_{2_1}.log_2 M_{2_1}G_3\left(\sqrt{\gamma_{1,A}}\right)\\ &+\frac{1}{2}M_{2_1}.log_2 M_{2_1}\left(\mathcal{G}_3\left(\sqrt{\gamma_{2,A}}\right)+\mathcal{G}_3\left(\sqrt{\gamma_{2,B}}\right)\right)\\ &+\frac{1}{2}M_{3_1}.log_2 M_{3_1}\left(G_3\left(\sqrt{\gamma_{3,A}}\right)+G_3\left(\sqrt{\gamma_{3,B}}\right)\right)\big].\end{aligned} \tag{94}$$

Substituting (93) and (94) into (86), we get N^{error}. As the next step, we should calculate N^{total}. This quantity can be calculated as

$$N^{total} = \sum_{k=1}^{3}\left(log_2 M_{1_k} + log_2 M_{2_k}\right)Pr(\gamma_1,\gamma_2,k) \tag{95}$$

where $Pr(\gamma_1,\gamma_2,k)$ denotes the probability that (γ_1,γ_2) belongs to the k-th region. This probability can be calculated as

$$Pr(\gamma_1,\gamma_2,k) = \int_0^{\infty}\int_0^{\infty}\Theta(\gamma_1,\gamma_2,k)p(\gamma_1)p(\gamma_2)d\gamma_1 d\gamma_2. \tag{96}$$

As explained in (89), given regions R_k, N^{total} can be divided into two parts for NU and FU as

$$N^{total} = N_1^{total} + N_2^{total}, \tag{97}$$

$$N_1^{total} = \sum_{k=1}^{3}\iint\left(log_2 M_{1_k} + log_2 M_{2_k}\right)p(\gamma_1)p(\gamma_2)d\gamma_1 d\gamma_2,$$

$$\gamma_1, \gamma_2 \in \mathcal{R}_k^1 \tag{98}$$

$$N_2^{total} = \sum_{k=1}^{3} \iint \left(log_2 M_{1_k} + log_2 M_{2_k}\right) p(\gamma_1) p(\gamma_2) d\gamma_1 d\gamma_2.$$

$$\gamma_1, \gamma_2 \in \mathcal{R}_k^2 \tag{99}$$

By limiting the $Pr(\gamma_1, \gamma_2, k)$ integral boundaries for $\mathcal{R}_k^1$ and $\mathcal{R}_k^2$ we have

$$Pr(\gamma_1, \gamma_2, k) = \int_{\beta_k}^{\infty} \int_{\alpha_k}^{\alpha_{k+1}} p(\gamma_1) p(\gamma_2) d\gamma_1 d\gamma_2 + \int_{\beta_k}^{\beta_{k+1}} \int_{\alpha_{k+1}}^{\infty} p(\gamma_1) p(\gamma_2) d\gamma_1 d\gamma e_2. \tag{100}$$

Therefore N^{total} can be written as

$$N^{total} = \sum_{k=1}^{3} \left(log_2 M_{1_k} + log_2 M_{2_k}\right) \times \left[\int_{\beta_k}^{\infty} \int_{\alpha_k}^{\alpha_{k+1}} p(\gamma_1) p(\gamma_2) d\gamma_1 d\gamma_2 + \int_{\beta_k}^{\beta_{k+1}} \int_{\alpha_{k+1}}^{\infty} p(\gamma_1) p(\gamma_2) d\gamma_1 d\gamma_2 \right]. \tag{101}$$

Given the Nakagami channel fading model, we can write this equation as

$$N^{total} = \sum_{k=1}^{3} \left(log_2 M_{1_k} + log_2 M_{2_k}\right) .e^{-\overline{\gamma_1 \gamma_2}} \left[e^{\frac{\alpha_k \beta_k}{\overline{\gamma_1}}} - e^{\frac{\alpha_{k+1} \beta_k}{\overline{\gamma_1}}} + e^{\frac{\alpha_{k+1} \beta_k}{\overline{\gamma_2}}} - e^{\frac{\alpha_{k+1} \beta_{k+1}}{\overline{\gamma_2}}} \right]. \tag{102}$$

Therefore, the closed-form of N^{total} based on the thresholds was calculated.

C. AVERAGE TRANSMISSION RATE

In the systems with adaptive modulation, because of changes in the modulation order according to SNR values, it is of high importance to calculate the average transmission rate.

By averaging the transmission rate over the system Modes, the average transmission rate can be calculated as

$$\begin{aligned} TR_{avg} &= \sum_{k=1}^{3} \iint T(M_{1_k}, M_{2_k}) p(\gamma_1) p(\gamma_2) d\gamma_1 d\gamma_2 \\ &= \sum_{k=1}^{\kappa} \int_{\beta_k}^{\infty} \int_{\alpha_k}^{\alpha_{k+1}} \left\{ \left(log_2 M_{1_k} + log_2 M_{2_k}\right) p(\gamma_1) p(\gamma_2) d\gamma_1 d\gamma_2 \right\} \\ &\quad + \sum_{k=1}^{\kappa} \int_{\beta_k}^{\beta_{k+1}} \int_{\alpha_{k+1}}^{\infty} \left\{ \left(log_2 M_{1_k} + log_2 M_{2_k}\right) p(\gamma_1) p(\gamma_2) d\gamma_1 d\gamma_2 \right\}. \end{aligned} \tag{103}$$

This can be expressed as a function of $\mathcal{F}_1$ as

$$TR_{avg} = \sum_{k=1}^{3} \left\{ log_2(M_{1k} + M_{2k}) \mathcal{F}_1(\Omega_1, \overline{\gamma}_1, \alpha_k, \alpha_{k+1}) \mathcal{F}_1(\Omega_2, \overline{\gamma}_2, \beta_k, \infty) \right\} + \sum_{k=1}^{3} \left\{ log_2(M_{1k} + M_{2k}) \mathcal{F}_1(\Omega_1, \overline{\gamma}_1, \alpha_k, \infty) \mathcal{F}_1(\Omega_2, \overline{\gamma}_2, \beta_k, \beta_{k+1}) \right\}. \tag{104}$$

which is the in closed-form for the average throughput.

VI. NUMERICAL RESULTS

In this section, the simulations for the adaptive modulation system are presented. First, we evaluate the results of the derivations of closed-form BER for different system operational Modes. Then, the evaluations of the average transmission rate and average BER are presented.

In our simulations, the variance of the fading coefficient ($\sigma^2 = E\{|h|^2\}$) is assumed to be d^{-l}, where d is the distance of the nodes from BS and $l = 5$ is the path loss exponent. Moreover, $\Omega_n = 1$, $BER_{target} = 10^{-2}$ and it is assumed that $c\text{SNR} = P_s/N_0$ is the reference signal-to-noise ratio where c is a constant and P_s is the total transmit power which we assume it to be equal to 1.

In addition, the comparison of the performance of the NOMA system over the OMA system is being extensively investigated such as [21], therefore, our aim is to focus on the comparison of the designed adaptive NOMA system over regular NOMA.

According to the simulations, the adaptive system has a better performance compared to the non-adaptive system. Also, the closed-form equations are following the simulation values with a high degree of accuracy.

A. SYSTEM OPERATIONAL MODES EVALUATION

In this subsection, we simulate different system operational Modes.

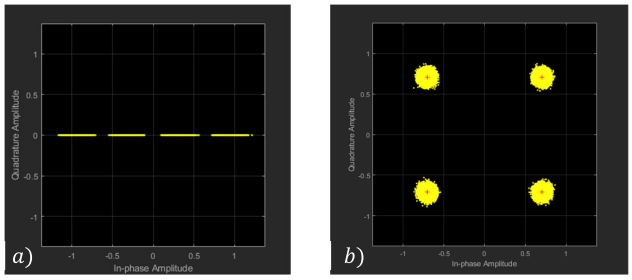

FIGURE 9. Constellation of the received symbols for Mode 1.

In Figure 9 a, one of the possible ways to have the constellation for Mode 1 is depicted. This includes the symbols for the NU and FU. As can be seen from the figure, the noise is only in the in-phase axis direction and there is no noise component in the quadrature axis. It is worth mentioning that these constellations refer to the symbols observed under real-world conditions, where the presence of noise and other impairments causes deviations from the ideal constellation points.

Figure 9 b shows another possible constellation for the first Mode of the system ($M_1 = 2$ and $M_2 = 2$) where the symbols of NU and FU are orthogonal. As can be seen

from the figure, since the symbols are orthogonal, the NU and FU users can utilize the I and the Q axis as their detection threshold respectively. It is worth mentioning that because of orthogonality, the in-phase noise component is not affecting SIC for NU.

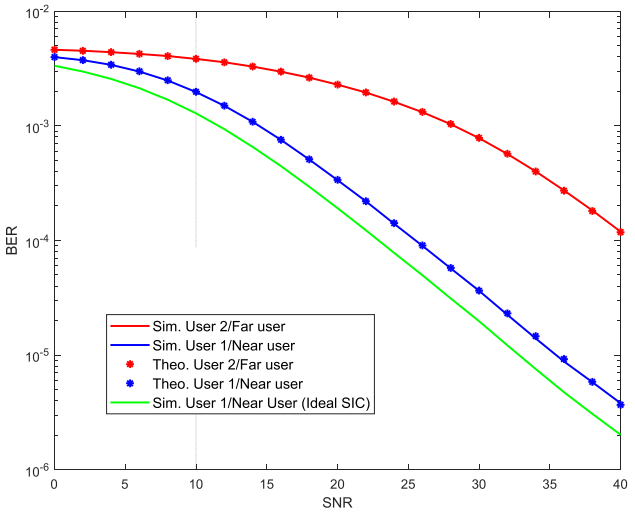

FIGURE 10. BER for NU and FU in Mode 1 for both analytical and theoretical cases.

In Figure 10, the BERs for NU and FU for both simulation and theoretical cases are plotted. In addition, the Ideal SIC process is also shown for the system which shows the difference between the ideal and non-ideal cases. The SNR on the horizontal axis represents the transmit SNR at the BS. Therefore, γ_1 and γ_2 can be determined based on the corresponding channel gain and power allocation factor.

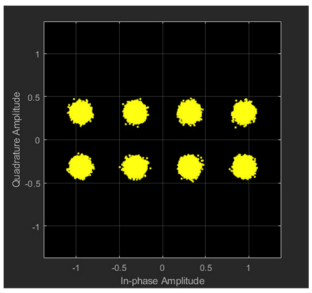

FIGURE 11. Constellation of the received symbols for Mode 2.

Figure 11 displays the constellation for Mode 2 where $M_1 = 4$ and $M_2 = 2$, therefore, the symbols have components in both axis. In this figure, the $I = 0$ line is the threshold for FU and NU will have to use two thresholds after the SIC process to decode the 4-QAM symbols. In addition, we set the power level values for near and far users as $\varepsilon_1 = 0.25$ and $\varepsilon_2 = 0.75$.

In Figure 12, analytical and theoretical analysis for Mode 2 is shown. As the figure shows, the simulation results match the theoretical ones. Clearly it can be seen that the simulation

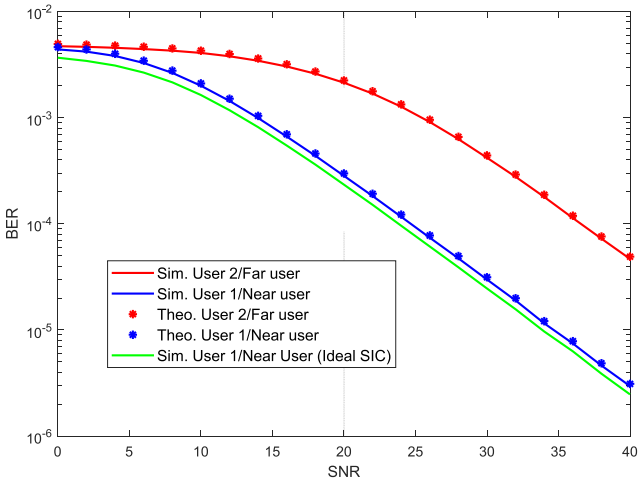

FIGURE 12. BER for NU and FU in Mode 2 comparing analytical and theoretical results.

values are close to the theoretical values which come from the closed-form functions.

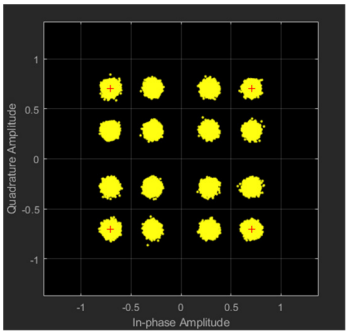

FIGURE 13. Constellation of the received symbols for Mode 3.

As we can see from Figure 13, the practical constellation of Mode 3 is shown for NU and FU where $M_1 = 4$ and $M_2 = 4$. It can be said that for FU, if the symbol is in one of the quarters of $I - Q$ axis, it represents a symbol for its 4-QAM constellation. In addition, NU should use two thresholds after SIC for its own 4-QAM demodulation. In addition, we set the power level values for near and far users as $\varepsilon_1 = 0.4$ and $\varepsilon_2 = 0.6$.

Figure 14 shows the investigation for BER which was made for state 3 of the system for all users. Also, for this system Mode, the values from the simulation and theory are in agreement.

B. ADAPTIVE SYSTEM EVALUATION

In this subsection, we investigate the proposed adaptive system using different criteria.

In Figure 15, the throughput of the system is depicted for different operational Modes versus different SNRs. As it can be understood from the figure, the throughput for the third system operational state is higher than the others since it uses higher-order modulations. One can say this Mode

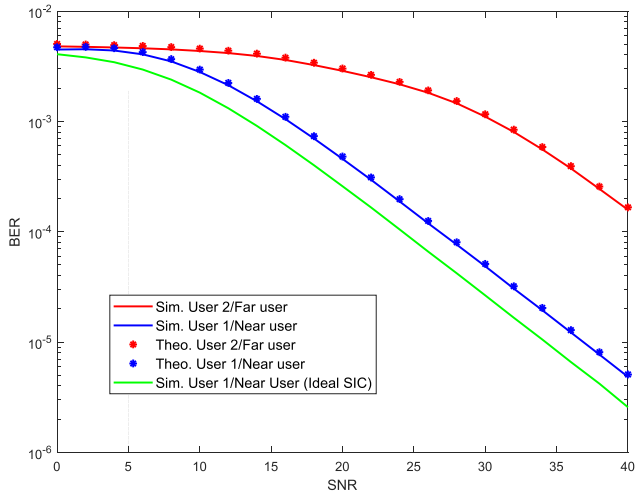

FIGURE 14. BER for NU and FU in Mode 3 for both simulation and theoretical cases.

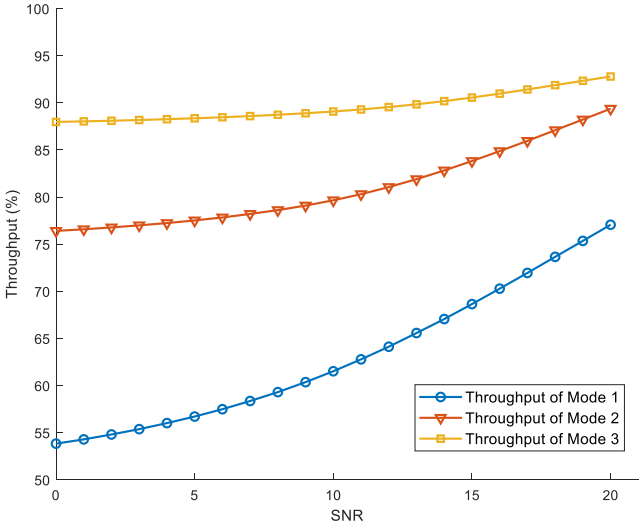

FIGURE 15. The throughput of the system for different operational Modes.

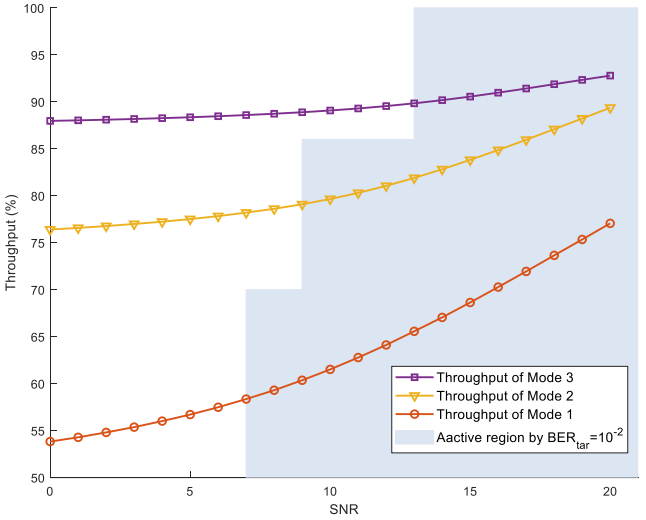

FIGURE 16. Active and deactivate regions considering the maximum acceptable $BER_{tar} = 10^{-2}$.

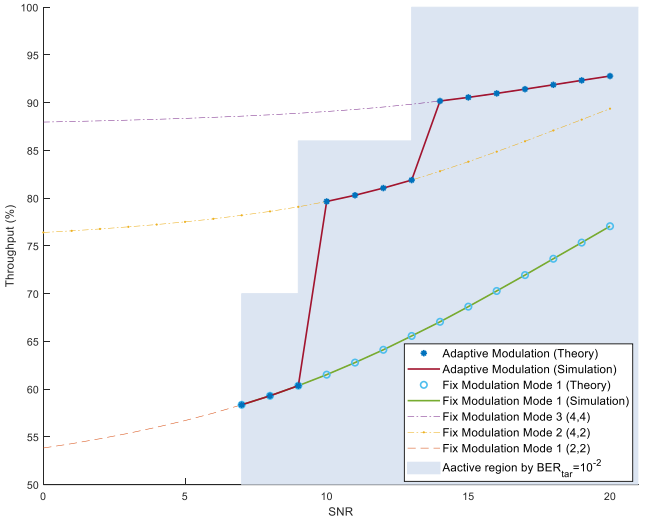

FIGURE 17. Throughput comparison between NOMA adaptive modulation and fix modulation NOMA for $BER_{tar} = 10^{-2}$.

can be always utilized for transmission and there is no need for an adaptive modulation system. However, it should be noted that there are different BERs for each Mode. Therefore, considering the acceptable BER threshold, each Mode can operate in a specific SNR range. The acceptable levels for BER which were presented in the previous section, can be transformed into transmit power levels. The active regions are shown in Figure 16.

It can be seen from Figure 16 that the active region for all operational Modes is depicted as a blue zone. In other words, the white zone states that for those SNR values in the related state, the BER constraint is not satisfied.

Figure 17 shows the throughput comparison between NOMA with adaptive modulation and fixed modulation for $BER_{tar} = 10^{-2}$. As the figure shows, the efficiency of the adaptive modulation system increases in comparison with the fixed modulation. The comparison of fixed modulation with the adaptive modulation system can be expressed as follows:

- *Case 1:* Adaptive modulation system comparison with fixed modulation ($M_1 = 2, M_2 = 2$): Both systems are activated together and by increasing the SNR, the fixed modulation system has less throughput as does not use the higher order modulations where the channel condition provides a suitable situation.
- *Case 2:* Adaptive modulation system comparison with fixed modulation ($M_1 = 4, M_2 = 4$): the fixed modulation system stays inactive until the BER constraint is met, therefore this system is unable to connect in lower SNR values. However, the adaptive system will start the communication with lower-order modulations. Hence, the adaptive system has better performance in terms of

transmission delay and bandwidth utilization. In higher SNRs, both systems operate equally.

- *Case 3:* Adaptive modulation system comparison with fixed modulation ($M_1 = 4$, $M_2 = 2$): In this case which is somehow the combination of cases 1 and 2, the adaptive system outperforms the fixed modulation in lower SNRs since it has the possibility to maintain the transmission as opposed to the fixed modulation case. Moreover, for higher SNRs, even though adaptive modulation uses a higher order modulation and therefore better throughput, the fixed modulation system still uses the same modulation order.

Considering all the cases above, one can be sure that the adaptive system performs better for different channel states which confirms the efficiency of the proposed scheme.

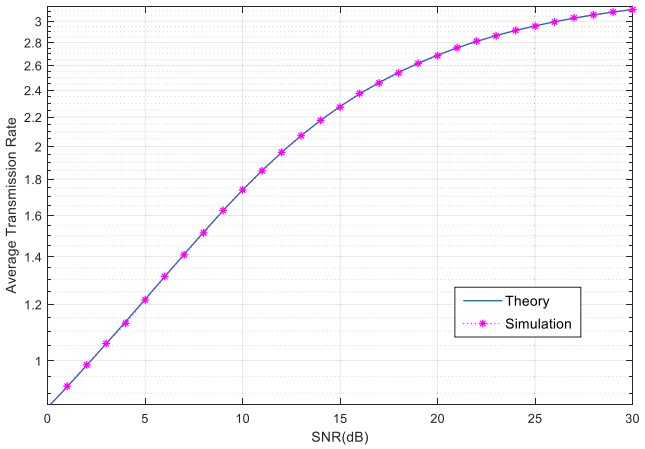

FIGURE 18. Average transmission rate for different SNRs calculated for theoretical and practical for $\alpha = 0.25$.

Figure 18 shows the average transmission rate for different SNRs calculated for theoretical and practical simulations. This figure verifies the increase in spectral efficiency by using the adaptive modulation system. In addition, the figure shows that the practical values match with the theoretical values.

Figure 19 displays the average BER for the adaptive modulation system. According to this figure, the simulations perfectly match the theoretical curves which verifies the validity of the derivations. It is worth mentioning that the system is considered to be delay-tolerant. The important thing which is shown in this figure is the fact that by spending the cost of increasing the BER (by using higher order modulations) while satisfying the BER constraint, the throughput of the system increased significantly.

In Figure 20, the average BER of the system is plotted versus different values of α for three SNRs. In this figure, α is in the range [0, 0.5]. The reason for this range is the fact that having $\alpha > 0.5$ means we assign more power to the NU which is contradictory with the NOMA principles and will result in invalid outputs. Moreover, as it was discussed before, if the channel state of the users changes in a way that the FU has a better channel state, the SIC process will be done in the

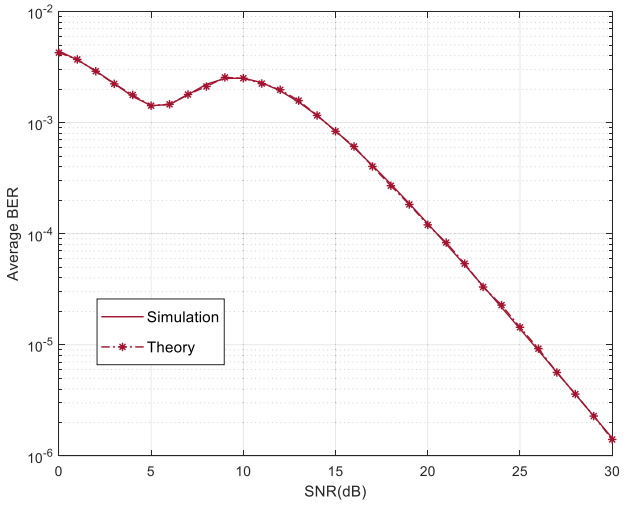

FIGURE 19. Average BER for different SNR values and $\alpha = 0.25$.

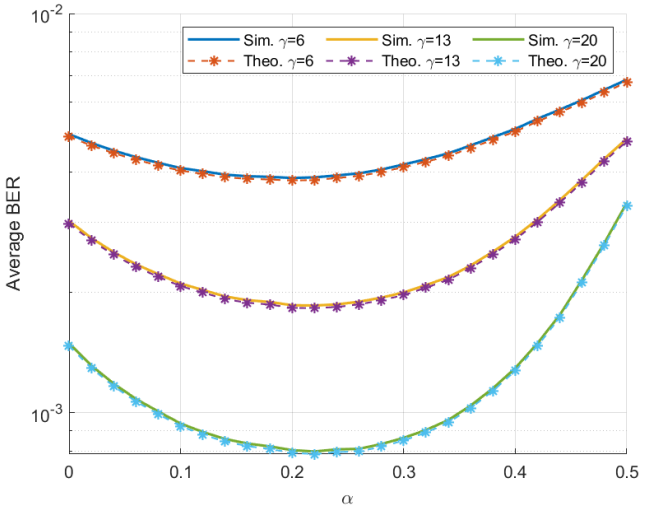

FIGURE 20. Average BER versus different α values.

FU receiver and NU will not be doing SIC anymore. In other words, the role of users will change. The other important thing about this figure is that we are able to detect and calculate the optimum value for α in order to have the minimum average BER.

In this section, we analyzed the proposed model by different simulations, it is clear that the exact BER models follow the theoretical ones and the adaptive modulation system provides better spectral efficiency and higher throughput.

VII. CONCLUSION

In this paper, a novel model for NOMA system with adaptive modulation was proposed to improve the system throughput. The BER derivations were provided for each user. We assumed the SIC process to be non-ideal and the results were compared with the ideal SIC. Then an optimization problem was formulated for the throughput with BER and power constraints. The solution was derived by determining

the thresholds for different system operational Modes and then the adaptation and alignment for the modulation in the downlink direction were done. Then the model was analyzed through different criteria such as average BER, throughput and average transmission rate using simulations. It was shown by the simulations that the adaptive NOMA system outperforms the NOMA system with fixed modulation. In other words, by introducing the cost of increasing the BER while maintaining the BER constraint for the maximum acceptable BER, the throughput of the system increases significantly. This greatly improves the spectral efficiency of NOMA systems and can be implemented in the networks serving a huge number of users to increase the Quality of Service (QoS).

APPENDIX A

$$
\begin{aligned}
&P_{3,1}\left(e|\textit{incorrect SIC}\right)\\
&= \frac{1}{4}\Pr\left(n_I \geq \sqrt{\varepsilon_2/2}|h_1| - \sqrt{\varepsilon_1/2}|h_1|\right)\\
&\quad\times\left\{\Pr\left(n_I \geq -2\sqrt{\varepsilon_2/2}|h_1| + \sqrt{\varepsilon_1/2}|h_1| \,|\, n_I \geq \sqrt{\varepsilon_2/2}|h_1| - \sqrt{\varepsilon_1/2}|h_1|\right)\right.\\
&\quad+\Pr\left(n_Q \geq -2\sqrt{\varepsilon_2/2}|h_1| + \sqrt{\varepsilon_1/2}|h_1| \,|\, n_I \geq \sqrt{\varepsilon_2/2}|h_1| - \sqrt{\varepsilon_1/2}|h_1|\right)\\
&\quad+\Pr\left(n_I \geq -2\sqrt{\varepsilon_2/2}|h_1| - \sqrt{\varepsilon_1/2}|h_1| \,|\, n_I \geq \sqrt{\varepsilon_2/2}|h_1| - \sqrt{\varepsilon_1/2}|h_1|\right)\\
&\quad\left.+\Pr\left(n_Q \geq -2\sqrt{\varepsilon_2/2}|h_1| - \sqrt{\varepsilon_1/2}|h_1| \,|\, n_I \geq \sqrt{\varepsilon_2/2}|h_1| - \sqrt{\varepsilon_1/2}|h_1|\right)\right\}\\
&\quad+\frac{1}{4}\Pr\left(n_I \geq \sqrt{\varepsilon_2/2}|h_1| + \sqrt{\varepsilon_1/2}|h_1|\right)\\
&\quad\times\left\{\Pr\left(n_I \geq -2\sqrt{\varepsilon_2/2}|h_1| + \sqrt{\varepsilon_1/2}|h_1| \,|\, n_I \geq \sqrt{\varepsilon_2/2}|h_1| + \sqrt{\varepsilon_1/2}|h_1|\right)\right.\\
&\quad+\Pr\left(n_Q \geq -2\sqrt{\varepsilon_2/2}|h_1| + \sqrt{\varepsilon_1/2}|h_1| \,|\, n_I \geq \sqrt{\varepsilon_2/2}|h_1| + \sqrt{\varepsilon_1/2}|h_1|\right)\\
&\quad+\Pr\left(n_I \geq -2\sqrt{\varepsilon_2/2}|h_1| - \sqrt{\varepsilon_1/2}|h_1| \,|\, n_I \geq \sqrt{\varepsilon_2/2}|h_1| + \sqrt{\varepsilon_1/2}|h_1|\right)\\
&\quad\left.+\Pr\left(n_Q \geq -2\sqrt{\varepsilon_2/2}|h_1| - \sqrt{\varepsilon_1/2}|h_1| \,|\, n_I \geq \sqrt{\varepsilon_2/2}|h_1| + \sqrt{\varepsilon_1/2}|h_1|\right)\right\}\\
&\quad+\frac{1}{4}\Pr\left(n_Q \geq \sqrt{\varepsilon_2/2}|h_1| - \sqrt{\varepsilon_1/2}|h_1|\right)\\
&\quad\times\left\{\Pr\left(n_I \geq -2\sqrt{\varepsilon_2/2}|h_1| + \sqrt{\varepsilon_1/2}|h_1| \,|\, n_Q \geq \sqrt{\varepsilon_2/2}|h_1| - \sqrt{\varepsilon_1/2}|h_1|\right)\right.\\
&\quad+\Pr\left(n_Q \geq -2\sqrt{\varepsilon_2/2}|h_1| + \sqrt{\varepsilon_1/2}|h_1| \,|\, n_Q \geq \sqrt{\varepsilon_2/2}|h_1| - \sqrt{\varepsilon_1/2}|h_1|\right)\\
&\quad+\Pr\left(n_I \geq -2\sqrt{\varepsilon_2/2}|h_1| - \sqrt{\varepsilon_1/2}|h_1| \,|\, n_Q \geq \sqrt{\varepsilon_2/2}|h_1| - \sqrt{\varepsilon_1/2}|h_1|\right)\\
&\quad\left.+\Pr\left(n_Q \geq -2\sqrt{\varepsilon_2/2}|h_1| - \sqrt{\varepsilon_1/2}|h_1| \,|\, n_Q \geq \sqrt{\varepsilon_2/2}|h_1| - \sqrt{\varepsilon_1/2}|h_1|\right)\right\}\\
&\quad+\frac{1}{4}\Pr\left(n_Q \geq \sqrt{\varepsilon_2/2}|h_1| + \sqrt{\varepsilon_1/2}|h_1|\right)\\
&\quad\times\left\{\Pr\left(n_I \geq -2\sqrt{\varepsilon_2/2}|h_1| + \sqrt{\varepsilon_1/2}|h_1| \,|\, n_Q \geq \sqrt{\varepsilon_2/2}|h_1| + \sqrt{\varepsilon_1/2}|h_1|\right)\right.\\
&\quad+\Pr\left(n_Q \geq -2\sqrt{\varepsilon_2/2}|h_1| + \sqrt{\varepsilon_1/2}|h_1| \,|\, n_Q \geq \sqrt{\varepsilon_2/2}|h_1| + \sqrt{\varepsilon_1/2}|h_1|\right)\\
&\quad+\Pr\left(n_I \geq -2\sqrt{\varepsilon_2/2}|h_1| - \sqrt{\varepsilon_1/2}|h_1| \,|\, n_Q \geq \sqrt{\varepsilon_2/2}|h_1| + \sqrt{\varepsilon_1/2}|h_1|\right)\\
&\quad\left.+\Pr\left(n_Q \geq -2\sqrt{\varepsilon_2/2}|h_1| - \sqrt{\varepsilon_1/2}|h_1| \,|\, n_Q \geq \sqrt{\varepsilon_2/2}|h_1| + \sqrt{\varepsilon_1/2}|h_1|\right)\right\}
\end{aligned}
$$

APPENDIX B

$$
\begin{aligned}
&P_{3,1}\left(e|\textit{incorrect SIC}\right) = \frac{1}{4}\\
&\Pr\left(\sqrt{\varepsilon_2/2}|h_1| - \sqrt{\varepsilon_1/2}|h_1| \leq n_I \leq 2\sqrt{\varepsilon_2/2}|h_1| - \sqrt{\varepsilon_1/2}|h_1|\right)\\
&\Pr\left(n_I \geq \sqrt{\varepsilon_2/2}|h_1| - \sqrt{\varepsilon_1/2}|h_1|\right)\Pr\left(n_Q \geq -2\sqrt{\varepsilon_2/2}|h_1| + \sqrt{\varepsilon_1/2}|h_1|\right)\\
&\Pr\left(\sqrt{\varepsilon_2/2}|h_1| - \sqrt{\varepsilon_1/2}|h_1| \leq n_I \leq 2\sqrt{\varepsilon_2/2}|h_1| + \sqrt{\varepsilon_1/2}|h_1|\right)\\
&+\Pr\left(n_I \geq \sqrt{\varepsilon_2/2}|h_1| - \sqrt{\varepsilon_1/2}|h_1|\right)\Pr\left(n_Q \geq -2\sqrt{\varepsilon_2/2}|h_1| - \sqrt{\varepsilon_1/2}|h_1|\right)\\
&+\Pr\left(\sqrt{\varepsilon_2/2}|h_1| + \sqrt{\varepsilon_1/2}|h_1| \leq n_I \leq 2\sqrt{\varepsilon_2/2}|h_1| - \sqrt{\varepsilon_1/2}|h_1|\right)\\
&+\Pr\left(n_I \geq \sqrt{\varepsilon_2/2}|h_1| + \sqrt{\varepsilon_1/2}|h_1|\right)\Pr\left(n_Q \geq -2\sqrt{\varepsilon_2/2}|h_1| + \sqrt{\varepsilon_1/2}|h_1|\right)\\
&+\Pr\left(\sqrt{\varepsilon_2/2}|h_1| + \sqrt{\varepsilon_1/2}|h_1| \leq n_I \leq 2\sqrt{\varepsilon_2/2}|h_1| + \sqrt{\varepsilon_1/2}|h_1|\right)\\
&+\Pr\left(n_I \geq \sqrt{\varepsilon_2/2}|h_1| + \sqrt{\varepsilon_1/2}|h_1|\right)\Pr\left(n_Q \geq -2\sqrt{\varepsilon_2/2}|h_1| - \sqrt{\varepsilon_1/2}|h_1|\right)\\
&+\Pr\left(\sqrt{\varepsilon_2/2}|h_1| + \sqrt{\varepsilon_1/2}|h_1| \leq n_I \leq 2\sqrt{\varepsilon_2/2}|h_1| + \sqrt{\varepsilon_1/2}|h_1|\right)\\
&+\Pr\left(n_Q \geq \sqrt{\varepsilon_2/2}|h_1| + \sqrt{\varepsilon_1/2}|h_1|\right)\Pr\left(n_I \geq -2\sqrt{\varepsilon_2/2}|h_1| + \sqrt{\varepsilon_1/2}|h_1|\right)\\
&+\Pr\left(\sqrt{\varepsilon_2/2}|h_1| - \sqrt{\varepsilon_1/2}|h_1| \leq n_Q \leq 2\sqrt{\varepsilon_2/2}|h_1| - \sqrt{\varepsilon_1/2}|h_1|\right)\\
&+\Pr\left(n_Q \geq \sqrt{\varepsilon_2/2}|h_1| - \sqrt{\varepsilon_1/2}|h_1|\right)\Pr\left(n_I \geq -2\sqrt{\varepsilon_2/2}|h_1| - \sqrt{\varepsilon_1/2}|h_1|\right)\\
&+\Pr\left(\sqrt{\varepsilon_2/2}|h_1| - \sqrt{\varepsilon_1/2}|h_1| \leq n_Q \leq 2\sqrt{\varepsilon_2/2}|h_1| + \sqrt{\varepsilon_1/2}|h_1|\right)\\
&+\Pr\left(n_Q \geq \sqrt{\varepsilon_2/2}|h_1| - \sqrt{\varepsilon_1/2}|h_1|\right)\Pr\left(n_I \geq -2\sqrt{\varepsilon_2/2}|h_1| + \sqrt{\varepsilon_1/2}|h_1|\right)\\
&+\Pr\left(\sqrt{\varepsilon_2/2}|h_1| + \sqrt{\varepsilon_1/2}|h_1| \leq n_Q \leq 2\sqrt{\varepsilon_2/2}|h_1| - \sqrt{\varepsilon_1/2}|h_1|\right)\\
&+\Pr\left(n_Q \geq \sqrt{\varepsilon_2/2}|h_1| + \sqrt{\varepsilon_1/2}|h_1|\right)\Pr\left(n_I \geq -2\sqrt{\varepsilon_2/2}|h_1| - \sqrt{\varepsilon_1/2}|h_1|\right)\\
&+\Pr\left(\sqrt{\varepsilon_2/2}|h_1| + \sqrt{\varepsilon_1/2}|h_1| \leq n_Q \leq 2\sqrt{\varepsilon_2/2}|h_1| + \sqrt{\varepsilon_1/2}|h_1|\right)\}
\end{aligned}
$$

REFERENCES

[1] S. K. Zaidi, S. F. Hasan, and X. Gui, "Evaluating the ergodic rate in SWIPT-aided hybrid NOMA," *IEEE Commun. Lett.*, vol. 22, no. 9, pp. 1870–1873, Sep. 2018.

[2] L. Bariah, S. Muhaidat, and A. Al-Dweik, "Error probability analysis of non-orthogonal multiple access over Nakagami-*m* fading channels," *IEEE Trans. Commun.*, vol. 67, no. 2, pp. 1586–1599, Feb. 2019.

[3] B. K. Ng and C.-T. Lam, "Joint power and modulation optimization in two-user non-orthogonal multiple access channels: A minimum error probability approach," *IEEE Trans. Veh. Technol.*, vol. 67, no. 11, pp. 10693–10703, Nov. 2018.

[4] A. Chauhan, S. Ghosh, and A. Jaiswal, "RIS partition-assisted non-orthogonal multiple access (NOMA) and quadrature-NOMA with imperfect SIC," *IEEE Trans. Wireless Commun.*, vol. 22, no. 7, pp. 4371–4386, Jul. 2023.

[5] Y. Iraqi and A. Al-Dweik, "Power allocation for reliable SIC detection of rectangular QAM-based NOMA systems," *IEEE Trans. Veh. Technol.*, vol. 70, no. 8, pp. 8355–8360, Aug. 2021.

[6] F. M. Caceres, K. Sithamparanathan, and S. Sun, "Theoretical analysis of hybrid SIC success probability under Rayleigh channel for uplink CR-NOMA," *IEEE Trans. Veh. Technol.*, vol. 71, no. 10, pp. 10584–10599, Oct. 2022.

[7] R. Zhang, H. Liu, S.-H. Leung, Y. Zhang, W. Tang, H. Wang, Z. Luo, and S. Roy, "Precoding design for multi-group MIMO-NOMA scheme with SIC residual analysis," *IEEE Trans. Veh. Technol.*, vol. 72, no. 4, pp. 4733–4750, Apr. 2023.

[8] H.-T. Chiu and F. Maehara, "Improper Gaussian signaling for two-user MISO-NOMA systems considering hardware impairments and imperfect SIC," *IEEE Access*, vol. 11, pp. 59827–59839, 2023.

[9] H. Jafarkhani, H. Maleki, and M. Vaezi, "Modulation and coding for NOMA and RSMA," *Proc. IEEE*, vol. 112, no. 9, pp. 1179–1213, Sep. 2024.

[10] T. Assaf, A. Al-Dweik, M. E. Moursi, and H. Zeineldin, "Exact BER performance analysis for downlink NOMA systems over nakagami-*m* fading channels," *IEEE Access*, vol. 7, pp. 134539–134555, 2019.

[11] F. Kara and H. Kaya, "Performance analysis of SSK-NOMA," *IEEE Trans. Veh. Technol.*, vol. 68, no. 7, pp. 6231–6242, Jul. 2019.

[12] F. Kara and H. Kaya, "BER performances of downlink and uplink NOMA in the presence of SIC errors over fading channels," *IET Commun.*, vol. 12, no. 15, pp. 1834–1844, Sep. 2018.

[13] M. Aldababsa, C. Goztepe, G. K. Kurt, and O. Kucur, "Bit error rate for NOMA network," *IEEE Commun. Lett.*, vol. 24, no. 6, pp. 1188–1191, Jun. 2020.

[14] E. M. Almohimmah and M. T. Alresheedi, "Error analysis of NOMA-based VLC systems with higher order modulation schemes," *IEEE Access*, vol. 8, pp. 2792–2803, 2020.

[15] A. J. Goldsmith and P. P. Varaiya, "Capacity of fading channels with channel side information," *IEEE Trans. Inf. Theory*, vol. 43, no. 6, pp. 1986–1992, Nov. 1997.

[16] A. J. Goldsmith and S.-G. Chua, "Variable-rate variable-power MQAM for fading channels," *IEEE Trans. Commun.*, vol. 45, no. 10, pp. 1218–1230, Oct. 1997.

[17] Y. Cai, Z. Qin, F. Cui, G. Y. Li, and J. A. McCann, "Modulation and multiple access for 5G networks," *IEEE Commun. Surveys Tuts.*, vol. 20, no. 1, pp. 629–646, 1st Quart., 2018.

[18] P. Schwenteck, G. T. Nguyen, H. Boche, W. Kellerer, and F. H. P. Fitzek, "6G perspective of mobile network operators, manufacturers, and verticals," *IEEE Netw. Lett.*, vol. 5, no. 3, pp. 169–172, Sep. 2023.

[19] A. F. M. S. Shah, A. N. Qasim, M. A. Karabulut, H. Ilhan, and M. B. Islam, "Survey and performance evaluation of multiple access schemes for next-generation wireless communication systems," *IEEE Access*, vol. 9, pp. 113428–113442, 2021.
[20] S. Gamal, M. Rihan, S. Hussin, A. Zaghloul, and A. A. Salem, "Multiple access in cognitive radio networks: From orthogonal and non-orthogonal to rate-splitting," *IEEE Access*, vol. 9, pp. 95569–95584, 2021.
[21] P. V. Reddy, S. Reddy, S. Reddy, R. D. Sawale, P. Narendar, C. Duggineni, and H. B. Valiveti, "Analytical review on OMA vs. NOMA and challenges implementing NOMA," in *Proc. 2nd Int. Conf. Smart Electron. Commun. (ICOSEC)*, Trichy, India, Oct. 2021, pp. 552–556.
[22] W. Yu, H. Jia, and L. Musavian, "Joint adaptive M-QAM modulation and power adaptation for a downlink NOMA network," *IEEE Trans. Commun.*, vol. 70, no. 2, pp. 783–796, Feb. 2022.
[23] T. Assaf, A. Al-Dweik, M. S. E. Moursi, and H. Zeineldin, "Efficient bit loading algorithm for OFDM-NOMA systems with BER constraints," *IEEE Trans. Veh. Technol.*, vol. 71, no. 1, pp. 423–436, Jan. 2022.
[24] H. Yahya, E. A. Alsusa, and A. Al-Dweik, "Min-max design and analysis of NOMA with adaptive modulation under BLER constraints," in *Proc. IEEE 96th Veh. Technol. Conf. (VTC-Fall)*, Sep. 2022, pp. 1–5.
[25] K. Wang, T. Zhou, T. Xu, H. Hu, and X. Tao, "Asymmetric adaptive modulation for uplink NOMA systems," *IEEE Trans. Commun.*, vol. 69, no. 11, pp. 7222–7235, Nov. 2021.
[26] J. Ni and J. Zheng, "Non-coherent grant-free NOMA through Pilot- and channel block-index modulation," *IEEE Wireless Commun. Lett.*, vol. 10, no. 4, pp. 705–709, Apr. 2021.
[27] F. Kara and H. Kaya, "On the error performance of cooperative-NOMA with statistical CSIT," *IEEE Commun. Lett.*, vol. 23, no. 1, pp. 128–131, Jan. 2019.
[28] G. Taricco, "Fair power allocation policies for power-domain non-orthogonal multiple access transmission with complete or limited successive interference cancellation," *IEEE Access*, vol. 11, pp. 46793–46803, 2023.
[29] J. Ding, J. Cai, and C. Yi, "An improved coalition game approach for MIMO-NOMA clustering integrating beamforming and power allocation," *IEEE Trans. Veh. Technol.*, vol. 68, no. 2, pp. 1672–1687, Feb. 2019.
[30] Y. Qit and M. Vaezi, "NOMA decoding: Successive interference cancellation or maximum likelihood detection?" in *Proc. 58th Annu. Conf. Inf. Sci. Syst. (CISS)*, Mar. 2024, pp. 1–6.
[31] A. H. Bastami and P. Halimi, "Asymmetric adaptive modulation with symbol-based network coding for heterogeneous two-way relay network," *IEEE Trans. Commun.*, vol. 67, no. 9, pp. 5996–6011, Sep. 2019.

MILAD HESHMATI received the B.Sc. degree from Isfahan University, Isfahan, Iran, in 2016, and the M.Sc. degree in telecommunication systems from the K. N. Toosi University of Technology, Tehran, Iran, in 2022. He is currently pursuing the Ph.D. degree in telecommunication systems engineering with the Department of Electrical Engineering, École de Technologie Supérieure (ÉTS), Montreal, Canada. His research interests include wireless network resource optimization, resource allocation, and non-orthogonal multiple access (NOMA) networks.

ALI H. BASTAMI received the B.S. degree from the University of Science and Technology, Tehran, Iran, in 2003, the M.S. degree from the Amirkabir University of Technology (Polytechnic), Tehran, in 2006, and the Ph.D. degree from the University of Tehran, Tehran, in 2011, all in electrical engineering. He joined the Faculty of Electrical Engineering, K. N. Toosi University of Technology, Tehran, in 2012, where he is currently an Associate Professor. His current research interests include wireless communications, with a focus on NOMA techniques, reconfigurable intelligent surfaces, energy harvesting and SWIPT, massive MIMO, cognitive radio, and cooperative networks.

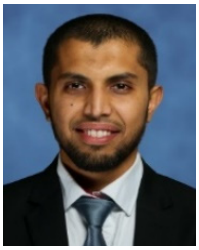

LOKMAN SBOUI (Senior Member, IEEE) received the Diplome d'Ingenieur degree (Hons.) in signals and systems engineering from the École Polytechnique de Tunisie (EPT), La Marsa, Tunisia, in 2011, and the M.Sc. and Ph.D. degrees in electrical engineering from the King Abdullah University of Science and Technology (KAUST), in 2013 and 2017, respectively. He was a Certification Analyst for mobile devices with Vidéotron, a Canadian telecom operator in Québec, from 2020 to 2021. Since 2021, he has been an Associate Professor with the Department of System Engineering, École de Technologie Supérieure (ÉTS), Montreal, Canada. His current research interests include energy efficiency and performance analysis of wireless communications, LEO satellites for the IoT, industrial automation and digital twins, urban air mobility (UAM), cognitive radio systems, and VoIP protocols. He has been with the IEEE Wireless Communications Letters Editorial Board, since 2021.

ZBIGNIEW DZIONG (Senior Member, IEEE) received the Ph.D. degree from Warsaw University of Technology, Poland. He was an Assistant Professor with Warsaw University of Technology. From 1987 to 1997, he was with the INRS-Telecommunications, Montreal, QC, Canada. From 1997 to 2003, he was with Bell Labs, Holmdel, NJ, USA. Since 2003, he has been with the École de Technologie Supérieure (University of Quebec), Montreal, as a Full Professor. He is an expert in the domain of performance, control, protocol, architecture, and resource management for data, wireless, and optical networks. He has participated in research projects for many leading telecommunication companies, including Bell Labs, Nortel, Ericsson, and France Telecom. He won the prestigious STENTOR Research Award, Canada, in 1993, for collaborative research. His monograph ATM Network Resource Management (McGraw Hill, 1997) has been used in several universities for graduate courses.